UPPSALA
UNIVERSITET

Digital Comprehensive Summaries of Uppsala Dissertations
from the Faculty of Pharmacy 312

Microgels as drug delivery vehicles

loading and release of amphiphilic drugs

YASSIR AL-TIKRITI

ACTA
UNIVERSITATIS
UPSALIENSIS
UPPSALA
2022

ISSN 1651-6192
ISBN 978-91-513-1502-7
URN urn:nbn:se:uu:diva-472818

Dissertation presented at Uppsala University to be publicly examined in Room A1:111a, BMC, Husargatan 3, Uppsala, Tuesday, 14 June 2022 at 09:15 for the degree of Doctor of Philosophy (Faculty of Pharmacy). The examination will be conducted in English. Faculty examiner: Professor Matthew Libera (Dept. of Chemical Engineering and Materials Science, Stevens Institute of Technology, Hoboken, NJ).

Abstract
Al-Tikriti, Y. 2022. Microgels as drug delivery vehicles. loading and release of amphiphilic drugs. *Digital Comprehensive Summaries of Uppsala Dissertations from the Faculty of Pharmacy* 312. 61 pp. Uppsala: Acta Universitatis Upsaliensis. ISBN 978-91-513-1502-7.

Polyelectrolyte microgels are used as delivery vehicles for amphiphilic drugs in, e.g., treatments of liver cancer by a method called trans-arterial chemoembolization. The thesis deals with fundamental properties of such delivery systems related to the self-assembling properties of the drug molecules and their interaction with the charged polymer network of the microgel. The main objective was to establish mechanistic models describing the loading and release of drugs under relevant conditions. For that purpose experimental techniques providing thermodynamic, compositional and microstructural information were used to elucidate how the kinetics depend on the stability of the drug self-assemblies and the volume response of the microgels. Micromanipulator-assisted microscopy studies showed that negatively charged microgels phase separated during loading and release of cationic amphiphilic drugs. At intermediate loading levels the drug aggregates and part of the network formed a collapsed phase coexisting with a swollen, drug-lean phase. In particular, during release in a medium of physiological ionic strength, the drug-lean phase formed a depletion layer (shell) surrounding a drug-rich core. Investigations of a series of drugs with different molecular architectures showed that the drug release rate was determined mainly by the stability of the drug aggregates in the core and the diffusive mass transport of drug molecules through the shell. Detailed studies of polyacrylate microgels interacting with amitriptyline hydrochloride showed that swelling of the shell network greatly influenced the release rate. Furthermore, experiments with a specially constructed microscopy cell was used to establish that the collapsed and swollen phases could coexist in equilibrium, and that the swelling of the network in the swollen phase depended on the proportion between them when present in the same microgel. The latter effect was related to the elastic coupling between the phases. Confocal Raman microscopy was employed to demonstrate, for the first time, the related elastic effect, that the concentration of amitriptyline in the swollen phase decreased with increasing proportion of the collapsed phase. Small-angle X-ray scattering showed that the collapsed phase had a disordered microstructure of drug micelles with ellipsoidal shape. The aggregation number increased with increasing concentration of drug in the microgel, most likely by incorporating the uncharged base form. By providing detailed information about thermodynamic properties and microstructures, the results of the thesis provide a basis for rational design of microgel drug delivery systems.

Keywords: microgel, amphiphilic drug, phase separation, micropipette, Raman microscopy, controlled release, drug delivery, SAXS

Yassir Al-Tikriti, Department of Medicinal Chemistry, Box 574, Uppsala University, SE-75123 Uppsala, Sweden.

ISSN 1651-6192
ISBN 978-91-513-1502-7
URN urn:nbn:se:uu:diva-472818 (http://urn.kb.se/resolve?urn=urn:nbn:se:uu:diva-472818)

To my family

"*When you reach the end of what you should know, you will be at the beginning of what you should sense*."

Khalil Gibran

List of Papers

This thesis is based on the following papers, which are referred to in the text by their Roman numerals.

I. Ahnfelt, E., Gernandt, J., **Al-Tikriti, Y.**, Sjögren, E., Lennernäs, H., Hansson, P. (2018) Single bead investigation of a clinical drug delivery system – A novel release mechanism. *Journal of Controlled Release*, *292*:235-247.

II. **Al-Tikriti, Y.**, Hansson, P. (2020) Drug-Eluting Polyacrylate Microgels: Loading and Release of Amitriptyline. *The Journal of Physical Chemistry B, 124* (11):2289-2304.

III. **Al-Tikriti, Y.**, Hansson, P. (2022) Drug-Induced Phase Separation in Polyelectrolyte Microgels. *Gels, 8* (1): 4.

IV. **Al-Tikriti, Y.**, Hansson, P. A small-angle X-ray scattering study of amphiphilic drug self-assemblies in polyacrylate microgels. *Manuscript*

V. **Al-Tikriti, Y.**, Edvinsson, T., Hansson, P. Elastic forces give rise to unusual phase transformations in polyelectrolyte gels: A Raman microscopy study. *Manuscript*

Other contributions not included in this thesis:

- Fagerberg, J. H., **Al-Tikriti, Y.**, Ragnarsson, G., Bergström, C. A. S. (2012) Ethanol Effects on Apparent Solubility of Poorly Soluble Drugs in Simulated Intestinal Fluid. *Molecular Pharmaceutics, 9* (7): 1942-1952.

Contents

Abbreviations

β	binding ratio
r	radius
ADI	adiphenine hydrochloride
AMT	amitriptyline hydrochloride
AMPS	acrylamide methylpropanesulfonate
$C_{12}TA^+$	dodecyltrimethylammonium ion
CAC	critical aggregation concentration
CCC	critical collapse concentration
CMC	critical micelle concentration
CPC	cetylpyridinium chloride
CPZ	chlorpromazine hydrochloride
C/S	swelled core/collapsed shell
DOX	doxorubicin
N_{agg}	aggregation number
PA	polyacrylate
R_{out}	microgel radius in the reference state
S/C	swelled shell/collapsed core
Span 60	sorbitane monostearate
SAXS	small angle X-ray scattering
TEMED	*N,N,N′,N′*-tetramethylethylenediamine
V/V_0	volume ratio

Introduction

Advances in drug discovery increase the need to develop novel delivery systems that offer protection to sensitive pharmaceutical substances, improve targeting and have the possibility to control the release process.[1-4] Such carriers help deliver drugs to the desired organs, improve their efficacy and reduce side effects. Especially for highly toxic active substances, encapsulating these molecules with the possibility for a local release at a specific organ would open up a new way to design new active pharmaceutical substances or even to reformulate already existing molecules. Biomacromolecules such as peptides and proteins are sensitive to denaturation.[5] They need a carrier system that protect them from degradation and maintain their native conformation. Microgels possess both chemical and mechanical properties that can be used to overcome these challenges.[6-14] They offer protection against denaturation. Here the nature of electrostatic interaction and water content inside the microgels help sensitive water-soluble biomacromolecules retain their native conformation and reduce the risk of aggregation. Electrostatic interactions facilitate loading large amounts of cationic amphiphilic drugs inside microgels.[15] Then the release process can be triggered by exposing the gel to different environmental stimuli such as pH or ionic strength.[16-22]

Doxorubicin, for example, is a cationic amphiphilic drug that is registered on the market as a cancer therapeutic.[23] DC beads are polymer microgels with a negative charge. Doxorubicin can be loaded in large amounts inside DC beads.[24-26] The loading process is accompanied by a decrease in the volume of the beads. After releasing the doxorubicin, they tend to swell. For the treatment of liver cancer, doxorubicin-loaded DC beads are applied locally by a catheter to the malignant cells in the liver.[27] The elevated ionic strength triggers the release process. Here the drug is released in a controllable manner. At the same time, the gels swell, causing the blood flow to the malignant tissue to stop, which provides a therapeutic dual effect. Embolization is beneficial to decrease the supply of nutrients to the tumour and at the same time, it limits the systemic spreading of the drug.

Much literature describes the chemical and pharmaceutical properties of microgels. But there is little information about the aggregation properties of the drugs inside the microgels and how self-assembly can affect the release profile. To predict the release profile of drugs from these gels with high accuracy, it is crucial to study the aggregation properties of the drugs together with

the mechanical properties of the microgels. In this work, we studied in depth the interaction between cationic amphiphilic drugs and oppositely charged microgels. In Paper I, we focused on the interaction between different cationic amphiphilic drugs and DC beads. We studied swelling and deswelling during loading and release. We also studied the importance of aggregation properties on the loading and release of doxorubicin. In Paper II, we used amitriptyline (AMT) as a model cationic amphiphilic drug and polyacrylate microgels as a model microgels delivery system. We studied the equilibrium properties at a low ionic strength while the kinetic properties, the loading and release, were studied both at a low and high ionic strength. In Paper III, we investigated in depth the stability of the phase separated state noticed in Paper II. One single microgel was equilibrated in a small volume of amitriptyline solution both at a low and high ionic strength to capture the intermediate phases. In Paper IV, we focused on the internal microstructure of polyacrylate microgels loaded with amitriptyline, doxepin and chlorpromazine (CPZ), respectively. A small-angle X-ray scattering technique was used to determine the shape of the aggregates and the aggregation number. In Paper V, we used Raman microscopy technique to analyze the composition of different parts of a single polyacrylate microgel loaded partially with amitriptyline at different loading levels.

Microgels

Microgels can be defined as soft and elastic spherical particles filled with water. They consist of permanently cross-linked polymer chains, in this work polyelectrolytes with negative charges. Microgels in this thesis can exhibit sizes from 10 μm to 1000 μm in diameter. They show volume responsiveness to environmental variations such as temperature, pH and ionic strength.[28]
Cross-linked polymer microgels are commonly used in drug delivery applications.[9, 29, 30] The electrostatic attractions between negatively charged microgels and oppositely charged cationic amphiphilic drugs facilitate loading large amounts of a drug inside these gels, with the added possibility of controlling the release process.[31-34] In addition, these gels can protect water-soluble biomolecules from denaturation.

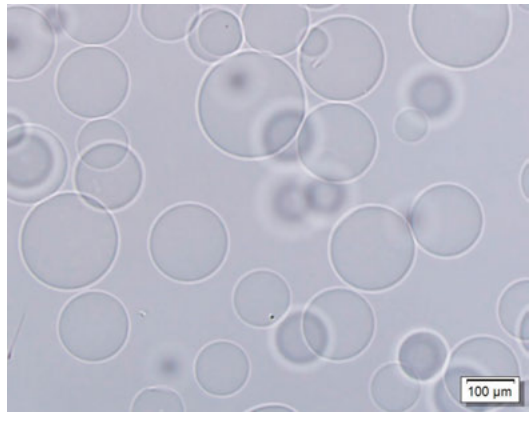

Figure 1. Polyacrylate microgels in water.

In this thesis I have used polyacrylate (PA) microgels consisting of slightly cross-linked polyacrylate chains with ~1.4 mol% cross-linker *N,N′*-methylenebisacrylamide. Since PA is a weak polyelectrolyte, the ionization degree is sensitive to pH. In this thesis, we used sodium phosphate buffer to keep the pH at 7.4 where the microgels are almost fully ionized. In an aqueous medium, polyelectrolytes dissociate into polyions and counterions.[35] The counterion entropy of mixing increases the osmotic pressure inside the gels and causes absorption of tremendous amounts of water, resulting in gel swelling,[36-38] see *Figure 1*. This means that, increasing the ionic strength of the solution surrounding the microgels decreases the volume of the gel. In addition, the elasticity of the gel network influences the swelling degree of the gel.[39-41] Increasing the degree of cross-linking reduces the swelling responsiveness of the gel.

We used the inverse suspension polymerization technique to form spherical microgels. The gels formed by this technique are polydisperse in size. In order to synthesize a more uniform size of microgels, the microfluidic technique can be used.

DC beads, sometimes referred to as microspheres or microgels, consist of polyvinyl alcohol segments integrated with chains containing negatively charged groups of AMPS.[42] These beads contain both charged and uncharged moieties. They are non-biodegradable which is beneficial for use as an embolic agent for the local treatment of liver cancer. Their volume responsiveness is lower than that of polyacrylate microgels, which simplifies theoretical analyses of drug release from them.

Biodegradable microgels can be interesting in subcutaneous drug delivery applications.[43] A commonly used class consists of cross-linked hyaluronate chains. At pH 7.4, the carboxylate groups are almost completely dissociated, possessing a negative charge. Hyaluronate microgels are not included in this

thesis but the conclusions from the polyacrylate microgels and DC beads facilitate building a theoretical model to predict the release profile for hyaluronate microgels.

Cationic amphiphilic drugs

Cationic amphiphilic molecules are typically characterized by the presence of a positively charged hydrophilic head group attached to a hydrophobic group of varying size and complexity,[44, 45] see *Figure 2*. They can be found in many drug classes registered on the market such as anticancer, antidepressant and antihypertensive drugs.

Understanding the mechanism of interaction between these drugs and oppositely charged microgels is necessary to design novel drug delivery carriers. Loading amphiphilic drugs causes the gels to deswell, while they swell again during the release process. Prior to this work, very little information existed about the aggregation properties and the distribution of cationic amphiphilic drugs inside microgels, and how these properties affect the release profile of a drug from microgels.

Efthymiou et al.[46] studied the aggregation properties of different amphiphilic molecules in water. They observed that all studied amphiphilic drugs formed small ellipsoidal micelles despite the differences in the properties of the hydrophobic part. This was in disagreement with previous work performed by Attwood et al.[44, 47, 48] with results based on classical techniques such as static light scattering and conductivity. Attwood suggested that molecules with flexible hydrophobic groups form closed micelles while the molecules with rigid ones form open aggregations that lack the well-defined critical micelle concentration. In this thesis we studied the aggregation properties of different amphiphilic drugs in PA microgels by using a small-angle X-ray scattering technique.

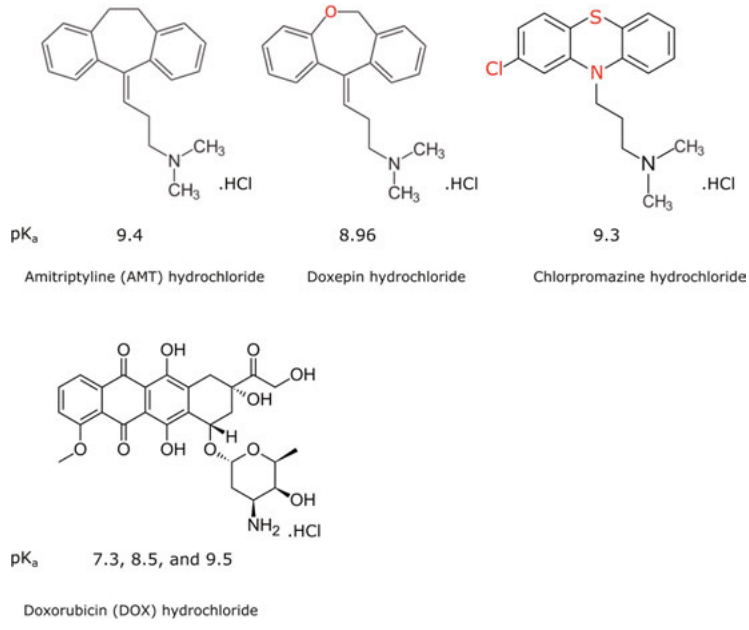

Figure 2. The chemical structures of different cationic amphiphilic drugs. pKa references: AMT,[49] doxepin,[50] chlorpromazine[51] and doxorubicin.[52]

CAC and CCC

The drug concentration needed to form micelles in a solution is called the critical micelle concentration (CMC). While the critical aggregation concentration (CAC) has been defined as a drug concentration in a solution in equilibrium with a gel, i.e. the concentration outside the gel needed to start forming micelles inside the gel.[53-56] The CAC value is usually much lower than the CMC value.[53, 57, 58] For example the CAC value for AMT is 0.37 mM (PA microgels) at an ionic strength of 10 mM, which is around 100 times lower than the CMC value, see Paper II. The reason for the difference between the two values was described earlier in a surfactant-polyelectrolyte system.[59] Surfactant molecules interact strongly with polyions of opposite charge. At a certain concentration, surfactant form micelles due to the hydrophobic effect. These micelles are stabilized by the polyions themselves and not the simple counterions. Compared with the binding of simple counterions the binding of polyions is associated with a smaller loss of entropy, and there is instead an entropic gain from the release of polyion counterions. This means the polyions induce and facilitate the formation of surfactant micelles at a concentration lower than CMC.

The critical collapse concentration, CCC, is the drug concentration needed to activate volume phase transition of the gel. The results in Paper II showed

that the CAC value was slightly lower than CCC. This means that a drug aggregation inside a gel is important but not sufficient to induce phase separation.

Phase transition in gels

Surfactant-microgel systems

Surfactant-gel systems have been studied extensively both experimentally and theoretically.[60-85] Nilsson et al.[86] studied the loading kinetics of dodecyltrimethylammonium ions ($C_{12}TA^+$) in polyacrylate microgels by using micromanipulation and light microscopy techniques. Here the volume transition was tracked during the loading process. A collapsed shell was formed surrounding a swollen core. They concluded that the surfactant diffusion through the stagnant layer in the liquid surrounding the microgel has a major role during the binding, and derived a theoretical deswelling model describing the volume changes during the loading process. The model was based on the assumption that the transport of surfactant from the liquid to the gel core was overall rate controlling, and that the gel was in osmotic equilibrium with its surroundings at every step of the binding process. The model described how variations in flow rate, surfactant concentration, CAC and gel size affected the rate of volume change, in satisfactory agreement with experiment.

Jidheden et al.[87] studied the equilibrium properties of $C_{12}TA^+$ in polyacrylate microgels. A single microgel was inserted in a small aqueous droplet enclosed inside an oil drop to prevent evaporation. Images were taken at specific intervals to track the changes in the gel. They observed phase separation in the microgels at a low ionic strength when the amount of surfactant in the droplet was smaller than that required to collapse the entire gel. A surfactant rich phase formed a dense shell outside the swollen gel core. The drawback of this technique is the presence of oil in contact with the system. Uncharged species of amphiphilic molecules may partition from the water phase to the oil. In Paper III, we developed a new technique where the system is not in contact with oil.

According to the theoretical calculations by Gernandt and Hansson,[88] the core/shell phase separation could be stabilized by limiting the amount of surfactant in the system. They found that, for solution-to-gel volume ratios below 200, the phase separated state represented the global free energy minimum of the model system. Under those conditions the surfactant concentration is sufficient to induce phase separation but the amount is not enough to fully load the gel.

In previous studies of equilibrium properties of microgels interacting with oppositely charged amphiphilic molecules, focus has been on phase separation

in a form of core/shell or shell/core pattern.[87, 88] In Paper III, we noticed a redistribution of the molecules to form another pattern of phase separation.

Understanding the behavior of the network and aggregation properties of oppositely charged amphiphilic molecules improves our understanding of the loading and release process. Therefore, it is important to investigate this interaction with clinically relevant cationic amphiphilic drugs.

Drug-microgel systems

Microgels can carry a large amount of oppositely charged drug inside. The electrostatic attractions facilitate drug diffusion into microgels, as an exchange with simple counterions.[18, 19] At a certain concentration, the drug molecules aggregate due to the hydrophobic effect.[89] The drug aggregates can be viewed as macroions interacting strongly with the polymer segments. The attraction between the segments and the oppositely charged drug causes a reduction in the volume of the gel that is larger than the reduction of the osmotic swelling pressure caused by the replacement of the network counterions,[90] as illustrated in *Figure 3*.

In general, there are two types of phase transition: continuous or discrete.[77, 91] In the continuous phase transition, the drug distributes evenly in the gel at all loading levels. The amount of drug uptake increases gradually with increasing free concentration on the liquid until reaching a fully collapse state.[87] In the discrete phase transition, the drug prefers to aggregate in one part of the gel at intermediate loading levels due to a net attractive interaction between drug aggregates. If there is enough supply of drug molecules (large solution volume) there is a jump in the gel volume at a critical drug concentration, and the collapsed part grows until reaching a homogenous fully collapsed state. The discrete phase transition in a surfactant-gel system was studied in depth in literature.[59, 74, 79, 92]

All the drugs studied in this thesis showed volume phase transition with intermediate states of phase separation. In Paper III we designed a new microscopy cell to study the stability of phase separation both at a low and high ionic strength. Phase separation usually occurs with hysteresis between loading and release.[93] Hysteresis in this case means that the concentration of drug in the solution where the collapse transition takes place is different from that where the swelling transition takes place.

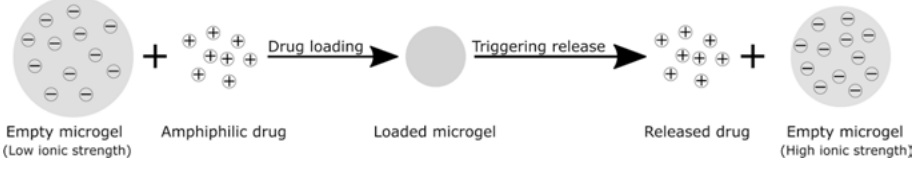

Figure 3. Schematic presentation of the interaction between a negatively charged microgel and an oppositely charged amphiphilic drug.

Cross-links and deformation

One of the main features that characterize microgels is cross-linking. The polyelectrolyte chains form a three-dimensional network. This means that any change in one part of the gel will affect the other parts. Microgels have a shape memory which makes them return to their original shape after deformation. The gel has a reference state where the network is relaxed. Any compression or extension from the reference state causes loss in the configurational entropy. By removing the external force, the gels return to their original form. The micelles formed inside microgels interact strongly with the network polyion chains. The gels have a tendency to phase separate into micelle-rich and micelle-lean domains due to polyion-mediated attractions between the micelles.[57, 94, 95] Coexistence of phases with different degree of swelling causes tensions in the network because of the cross-linking, and the collapsed part affects the swelled part, and vice versa.

Gernandt and Hansson[93] described theoretically, in an illustrative way, the relationship between the collapsed and swelled parts. The gel was divided into uniform volume elements. At the interface between the core and the shell, the network on the collapsed and the swelled side need to adapt to each other. In the case of collapsing a swelled gel, the new phase forms in the outer layer of the gel as a shell.[96] Here the shell elements in contact with the swollen elements need to stretch biaxially to fit the swollen elements. The stretching is followed by relaxation in the radial direction. In this way the composition in the deformed elements remains almost the same as the original composition before deformation. In the case of swelling a collapsed gel, the swollen shell elements in contact with the core are compressed biaxially to fit the collapsed core elements, followed by a radial relaxation. But in this case, these elements do not return to the original composition. Understanding the difference between the cost of deformation of the core/shell (C/S) during the loading process and the shell/core (S/C) during the release process, is important to predict the loading and release profiles accurately.

Aims of the thesis

The overall aim of my work is to improve understanding of the mechanism of interaction between cationic amphiphilic drugs and oppositely charged microgels. In specific, to understand how the self-assembling properties of the drug and the volume responsiveness of the microgels affect the drug loading to and release from microgels.

- **Paper I**: To provide a mechanistic understanding of the loading and release profile of different cationic amphiphilic drugs in DC beads microgels.
- **Paper II**: To improve the fundamental understanding of the loading and release profile of cationic amphiphilic drugs in microgels. We investigated the interaction of amitriptyline in polyacrylate microgels, experimentally and theoretically, from an equilibrium and kinetic perspective.
- **Paper III**: To investigate if the sharp boundary between the core and the shell observed in polyacrylate microgels during amitriptyline loading and release is stabilized thermodynamically or kinetically.
- **Paper IV**: To study the aggregation properties of different cationic amphiphilic drugs in polyacrylate microgels by using a small-angle X-ray scattering technique.
- **Paper V**: To investigate the composition of different parts of a polyacrylate microgel at intermediate drug loads by using a Raman microscopy technique.

Methods

Gel synthesis

Microgels

Polyacrylate microgels were synthesized in our lab by the inverse suspension polymerization technique.[86, 87, 97] The aqueous phase consisted of a mixture of acrylic acid, cross-linker *N,N′*-methylenebisacrylamide (1.4 mol% of the total amount of monomers), accelerator TEMED, sodium hydroxide and water, while the organic phase was composed of a mixture of Span 60 and cyclohexane. The organic phase was added to a two-neck flask under a nitrogen atmosphere to prevent the oxygen from dissolving in the mixture. The flask was heated to 45 °C under 400 rpm stirring. The aqueous phase was activated by adding ammonium persulfate (initiator). Immediately after activation, the aqueous phase was injected stepwise into the organic phase. The temperature was raised to 60 °C and the stirring was increased to 1000 rpm. After 30 min, the reaction was stopped by adding methanol. The resulted microgels were removed and dried in a Carbolite Furnaces airflow oven at 60 °C. Then the dried microgels were suspended in water and rinsed a few times with water. The pH was controlled to be ca. 9. The microgels were stored in a refrigerator. With this technique, the resulting microgels were polydisperse with diameter sizes ranging from 10 μm to 1000 μm. Sieves with different pore sizes were used to collect the desired gel size.

DC beads (100-500 μm diameter) were purchased from Biocompatible, UK and used as received.

Macrogels

Polyacrylate macrogels were synthesized by mixing acrylic acid, cross-linker *N,N′*-methylenebisacrylamide (1.4 mol% of the total amount of monomers), accelerator TEMED, and ammonium persulfate in water. The solution was degassed and poured into small glass tubes and then heated for 3 h at 65 °C. The macrogels were stored overnight in a 0.5 M sodium hydroxide solution. After that, the resulting macrogels were rinsed with water three times with 24 h interval between each rinse. The pH was kept at ~ 9.

Solution preparation

In Paper I, we used water as a medium to dissolve amphiphilic drugs and to study the loading process, while 150 mM NaCl salt was used to trigger the release process. In Paper II-V, we used sodium phosphate buffer to keep the pH of the system at 7.4. The ionic strength during loading was 10 mM (5 mM phosphate buffer + 5 mM NaCl) while during the release process the ionic strength was raised to 155 mM (5 mM phosphate buffer + 150 mM NaCl).

Microgel charge density

We used a Mettler Toledo MT5 microbalance to weigh freeze-dried polyacrylate microgels. The remaining moisture inside the microgels, after freeze-drying, was determined by using a differential scanning calorimeter (DSC Q 2000, TA instrument). The weighed gels were suspended in water in a microscopy cell designed in our lab to measure the diameter of all the gels. The cell was placed in a light microscope and multi-images were taken to include all the gels inside the cell. From the diameter of the microgels, we calculated the total volume of all the gels. Finally, the average concentration of the polyacrylate segments in microgels was measured by dividing the weight of the freeze-dried polyacrylate microgels by the total volume of the gels.

Loading and release experiments

The collapse/swelling of a single microgel during drug loading and release, respectively, were studied experimentally by using a micromanipulator-assisted light microscopy technique. In this technique, we were able to track the volume changes of a single microgel, and monitor the distribution of the drug inside the gel during loading and release. A micropipette was used to hold a single microgel with a desired volume, as illustrated in *Figure 4*. The gel was inserted inside a flow pipette under controlled conditions. Images were taken at specific intervals to investigate the intermediate phases during the loading and release process. We varied the flow rate, size of the gel and drug concentration in the solution that flowed in the pipette to analyse the transport process. The detailed setup can be found in Paper II. This method provides quantitative information regarding the loading and release process.

We investigated the distribution of the drug inside the gel by using a fluorescence microscopy technique. Rhodamine B was used as a hydrophobic probe to track the distribution inside the gel. This probe distributes in the hydrophobic part of the drug micelles. As a result, the intensity of the color inside the gel reflects the concentration of the drug micelles in the gel.

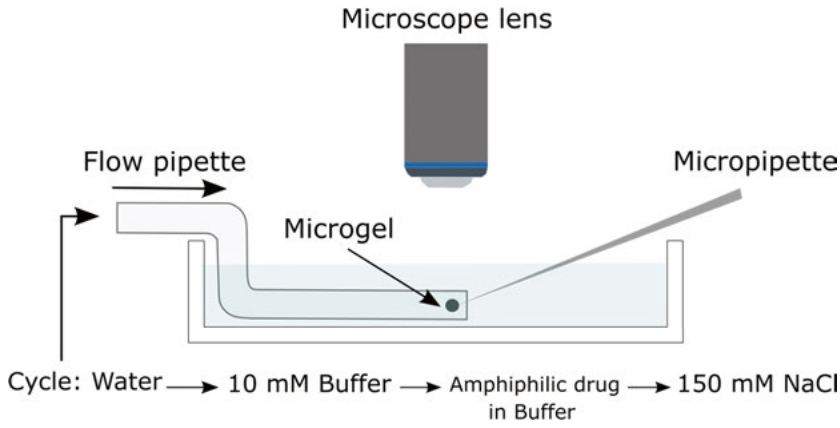

Figure 4. Schematic illustration for the micromanipulator-assisted light microscopy technique.

Binding isotherms

Here we studied the binding isotherms for AMT in both polyacrylate microgels and macrogels. In principle, we dissolved a certain amount of AMT in a dispersion of microgels. The amount was chosen to cover the intermediate loading levels. After equilibration, the concentration of AMT in the solution in equilibrium with the microgels was measured by UV absorption spectroscopy using a μDISS profiler (Pion Inc.). This instrument provides concentration measurements with high accuracy. The binding ratio β, which represents the molar ratio of AMT to polyacrylate segments in the microgels, was calculated by the following equation

$$\beta = \frac{C_{AMT}^{total} - C_{AMT}^{free}}{C_{PA}^{gel}} \quad (1)$$

where C_{AMT}^{total} represents the total concentration of AMT in the system, C_{AMT}^{free} represents the concentration of AMT in the solution outside the microgels and C_{PA}^{gel} represents the concentration of PA segments in the microgels.

We used the same technique to measure the binding isotherm of AMT in systems of polyacrylate macrogels. The only difference is that we equilibrated one macrogel with AMT instead of a microgels dispersion.

Swelling isotherms

We studied the swelling isotherms for a single polyacrylate microgel in AMT solution at 10 mM and 155 mM ionic strength. Equilibrating one single microgel (diameter: 100-1000 µm) in a small volume of a drug solution (3-15µl) needs a special setup. Here, we designed a new microscopy cell that enables us to equilibrate a single microgel in a small volume of AMT solution, as presented in *Figure 5*. The cell consists of a glass tube attached to a petri dish. At 10 mM ionic strength, the gel was selected and positioned in the tube by using a micro holder. Then the tube was sealed to prevent evaporation. To avoid optical reflections, the petri dish was filled with water. Images were captured to investigate the volume change at different loading levels and distribution of AMT inside the gel. The binding ratio was calculated by using equation 1.
At 155 mM ionic strength we used a slightly different approach. First, the gel was loaded with AMT by inserting the gel in 0.7 mM AMT solution at 10 mM ionic strength overnight. Then the loaded gel was moved to a small volume of AMT solution at 155 mM ionic strength. Different loading levels could be captured by controlling the volume and the concentration of AMT solution. After 5 h equilibration time, we captured images of the gels to analyze the volume changes and drug distribution. The amount of AMT inside the gel was measured by moving the gel, after equilibration, to a 250 µl buffer solution and its concentration was measured by a µDISS profiler. The number of moles of AMT was divided by the number of moles of acrylate segments in the gel to get the binding ratio. As far as we know, this is the first experimental study to investigate the swelling isotherm for an amphiphilic drug in a single microgel at physiological ionic strength.

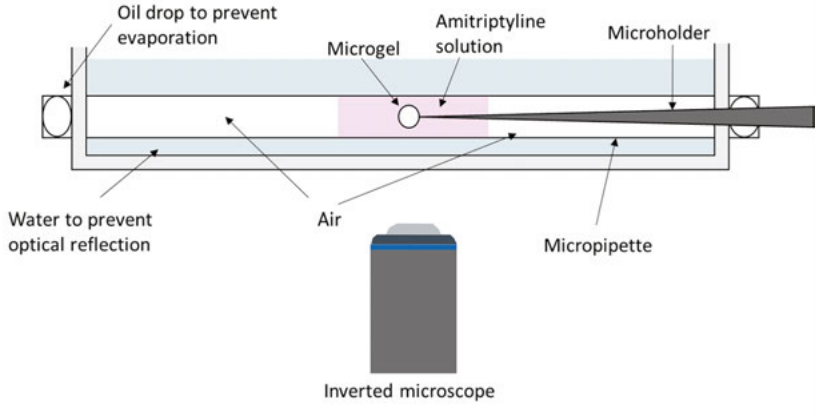

Figure 5. Schematic illustration of the small-volume microscopy cell setup.

Drug concentration inside the gel

We measured the concentration of AMT, chlorpromazine (CPZ) and doxepin in a single microgel to investigate the sensitivity of fully collapsed gels to different drug concentrations in the solution. The gel was equilibrated in a drug solution of a certain concentration overnight and images were captured to determine the size of the gel after reaching a fully collapsed state. Then the gel was moved to a 250 µl buffer solution to release its cargo. The concentration of the drug in the buffer solution, which corresponded to the amount of the drug initially inside the gel, was measured by using a µDISS profiler equipped with a 20 mm probe. The measured drug amount was divided by the volume of the gel after equilibration to get the concentration inside the gel.

Theoretical models for release

Gel model

In paper II we used a mean-field model to calculate the composition of the microgel. The microgel was considered to consist of a solution of monovalent anions and cations, a polymer network, water, and drug micelles in equilibrium with drug monomers. The total free energy of the gel was described as a sum of the free energy of mixing, electrostatic free energy, a transfer free energy, and the elastic deformation energy of the network. The calculations of the entropy of mixing took into account excluded volume interactions between micelles. The electrostatic energy was based on a capacitor model for polyion-mediated attractions between micelles. The transfer free energy describes the hydrophobic effect, mainly the non-electrostatic free energy of transferring drug monomers into a micelle. In the case of a microgel with a collapsed core surrounded by a swollen shell, the deformation of the network in the shell is anisotropic and depends on the radial position. Therefore, the lateral and radial strains were calculated based on the current position in relation to the position in a reference state.[76]

Release model

In a fully loaded microgel, the drug distributes evenly forming aggregates in equilibrium with drug monomers. Moving the gel to drug-free solution of 155 mM ionic strength triggers the release. The model calculations were based on the intraparticle diffusion-controlled mechanism. Here the salt enters the gel within a few seconds. Thereafter the drug aggregates dissolve in the outer layer forming a swelled part (shell) in contact with a collapsed one (core). The concentration of the drug outside the gel can be set to zero because of the sink condition. The release model is based on the presence of a sharp boundary

between the core and shell, a depletion-layer model. Here the concentration gradient of the monomer between the inner and outer layer of the shell, the diffusion coefficient and the thickness of the shell are assumed to determine the release rate. During the release process, the core decreases in size while the shell expands. Here inward and outward growth of the shell can be observed. The inward growth is due to the dissolution of the aggregates in the core. This means the shell grows at the expense of the core. The outward growth is caused by the swelling the gel network where the shell expands as drug aggregates dissolve.

The moderate volume change observed experimentally between the collapsed and the swollen states of DC beads, justifies assuming a fixed gel volume in the theoretical release calculation. Thus in the model of Paper I, the increase of the shell thickness was attributed only to the shrinking of the core. However, due to the very high responsiveness of polyacrylate microgels, we needed to include the volume change of the gel in the calculations in Paper II.

Small-angle X-ray scattering technique

Small angle X-ray scattering (SAXS) is a powerful analytical technique to investigate microstructures in colloidal systems. In principle, an X-ray radiation source with a low wavelength is transmitted through the sample. The resulting X-rays are collected on a detector where the scattering pattern contains information about the electron density distribution in the sample, and therefore about the spatial distribution of molecules and molecular assemblies. From the scattering angle, we calculate the scattering vector $q = \frac{4\pi\sin(\theta)}{\lambda}$ where the λ represents the wavelength of the X-ray source, which for CuK_{α} is 1.54Å, and 2θ represents the scattering angle.[98] A Xeuss 2.0, Xenocs X-ray system was used to investigate the microstructure of drug-loaded microgels. Freeze-dried microgels were equilibrated in solutions with different concentrations of AMT, chlorpromazine and doxepin. The fully loaded gel slurry was mounted on a gel holder and positioned at 270 mm from the detector. The background scattering from the solution in equilibrium with the gels was subtracted from the raw scattering of the gel sample by the data reduction routine in the XSACT 2.4 software. The resulting curves represent the scattering from the drug-microgel complexs. The scattering intensities were plotted as a function of q and analyzed using SasView 4.2.2 software. A scattering model using a core-shell ellipsoid form factor[99, 100] combined with a Hayter-Penfold Rescaled Mean Spherical Approximation (RMSA) structure factor[101, 102] could be fitted to the all recorded SAXS curves. The volume of the micelle was calculated by using the equation $V_{mic} = \frac{4\pi r_{equatorial}^2 \, r_{polar}}{3}$. The aggregation number N_{agg} was calculated by dividing the total volume of a micelle by the volume of a single drug molecule.

Raman microscopy technique

Raman microscopy merges Raman spectroscopy with microscopy technique. It is an analytical method commonly used in pharmaceutical development processes to investigate the chemical composition of a dosage form. It is a laser-based technique where the resulting spectra depend on the vibrational mode of molecules.[103] The spatial resolution is typically in the range of a few micrometres which permits investigating different spots inside the microgels used in this thesis. In paper V, the Raman microscopy technique was used to study the concentration of AMT in specific parts of partially loaded PA microgels. First, we designed a microscopy cell suitable for the Raman microscope. Briefly, we fixed a glass tube, 1.5 mm diameter, in a well plate. Then we selected a single gel by using a gel holder which was attached to a microinjector. The gel holder was detached from the injector and was fixed inside the glass tube. Here the gel was equilibrated in a small volume of AMT solution. The new setup offered the possibility to move the cell freely without the need to be attached to the injector. The measurements were performed on a Renishaw Qontur Raman spectrometer using a 785 nm laser and a 1200 lines/mm grating. The system was calibrated with a Si reference with the pronounced vibration mode at 520.5 cm^{-1}. We compared the intensity of the spectra between different microgels with variety of loading levels and between different spots in phase separated microgels.

Results and discussion

Gel characterization

Polyacrylate microgels were exposed to different electrolyte concentrations (buffer + NaCl) to characterize volume responsiveness to ionic strength. The results showed that the average gel volume per mole of carboxylate groups decreased from 0.015 m^3/mol in water to 0.004 m^3/mol in 155 mM ionic strength buffer (5 mM phosphate buffer + 150 mM NaCl, pH 7.4). Different gels in a variety of sizes showed almost the same swelling properties, which revealed homogeneity between microgels in their network structures, see *Figure 6A*.

Freeze-drying of polyacrylate microgels did not affect the stability of the network. After dispersion in water, they regained their spherical shape. The swelling was reversible and the microgels were stable after exposure to different electrolyte concentrations. Polyacrylate macrogels and microgels showed a similar swelling response to changes in electrolyte concentration as shown in *Figure 6B*.

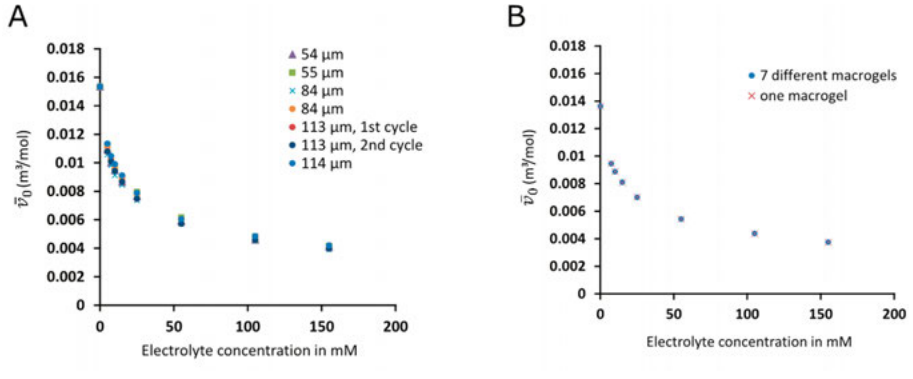

Figure 6. Volume responsiveness of PA gels in electrolyte solutions. A) Microgel volume, per mole of carboxylate groups, in different electrolyte concentrations. The legend represents the radius of each microgel in 5 mM buffer. B) Macrogel volume, per mole of carboxylate groups, in different electrolyte concentrations.

Equilibrium properties at 10 mM ionic strength

In Paper II, we investigated the interaction between AMT and PA macro- and microgels by means of binding and swelling isotherms. The binding isotherms describe the relationship between the loading levels of a drug inside the gel and the free drug concentration which the gel is in equilibrium with, while the swelling isotherms describe the changes in the volume of the gel in response to the binding ratio or the free drug concentration.

Microgels

A suspension of PA microgels were equilibrated with AMT for 6 weeks. The binding isotherm revealed that, above a critical aggregation concentration, the drug started to load onto the microgels cooperatively until all gels were homogenous and fully collapsed. The binding isotherm, as shown in *Figure 7A,* can be divided into three regions, the transition points between them are indicated with arrows.

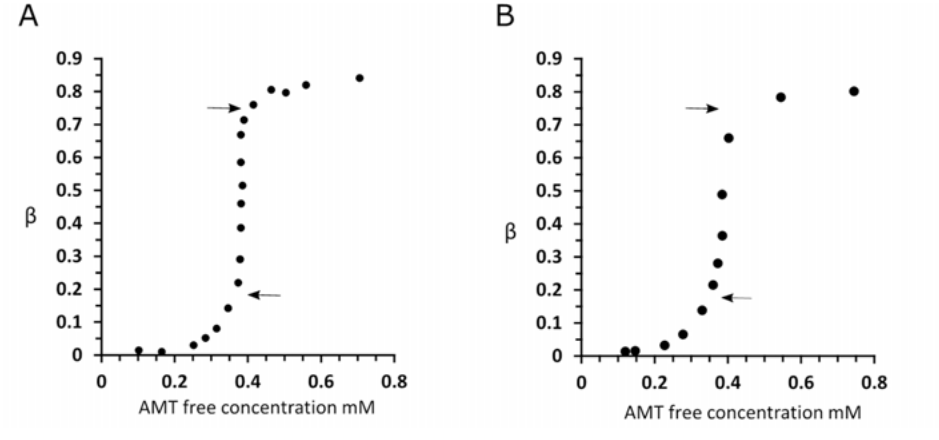

Figure 7. Binding isotherms of AMT in PA microgels (A) and macrogels (B). Arrows represent the transition point between different regions. β is the binding ratio and AMT free represents the equilibrium concentration of AMT.

The first region is accompanied by low loading levels. Here the binding ratio increases gradually with increasing concentration of free drug. The microscope images showed no sign of phase separation but the slope of the curve indicated the presence of drug aggregates inside microgels.[104]

The second region started at β ~0.22. The binding ratio increased sharply with increasing amount of added AMT while the free AMT concentration (outside the gels) remained almost constant. The images in this part revealed the presence of collapsed gels in equilibrium with swelled ones, see *Figure 8*. One interesting finding was that, at intermediate loading levels, the drug preferred to aggregate in one gel until it was fully collapsed while leaving the

other gels swelled. Raising the loading concentration increased the proportion of collapsed gels to swollen ones. We believe no one has reported this type of distribution earlier, i.e., of collapsed and swollen gels in the same system.

The third region starts when all the gels are fully collapsed. The binding ratio increased slightly with increasing AMT concentration, which indicates non-cooperative binding.

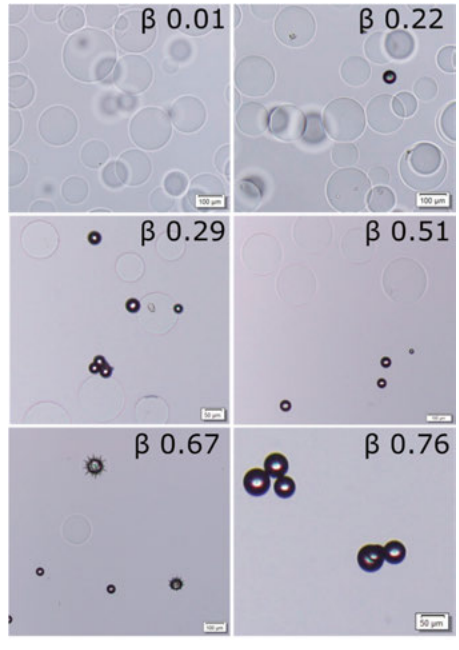

Figure 8. Light microscopy images of suspension of PA microgels equilibrated in AMT solution at 10 mM ionic strength. β is the binding ratio that represents the loading level inside the gel. The dark spheres are collapsed PA microgels fully loaded with AMT.

Macrogels

Single cylinder-shaped macrogels were equilibrated in AMT solutions for 8 weeks. The binding isotherm presented the same regions as in the microgels system, see *Figure 7B*. In the first region, the gel decreased in size with no sign of phase separation. The slope of a log-log curve in this region is larger than 1 for $\beta > 0.02$. In addition, the swelling isotherm for the macrogel-AMT system, in the same region, showed a decrease in the volume of the gel, see *Figure 9*. This indicates the presence of drug aggregates inside the gel before phase separation. We concluded that AMT aggregation inside the gel was important but not sufficient to induce phase separation. Phase separation started at $\beta \sim 0.22$, marking the transition to the second region, where the binding was

cooperative until the whole gel was fully collapsed. The difference between the microgels and the macrogel systems is that the latter contains only one macrogel instead of a suspension of microgels. Here the collapsed phase appeared in the outer layer of the gel, forming a core/shell pattern.

Notice the dramatic change in drug concentration inside the gel between the highest loading level in the first region and the third region. In the first one, the drug concentration was 0.029 M while the drug concentration inside the macrogels at the beginning of the third region was around 1.8 M. This reveals a huge loading capacity of these gels which can be beneficial in drug delivery applications.

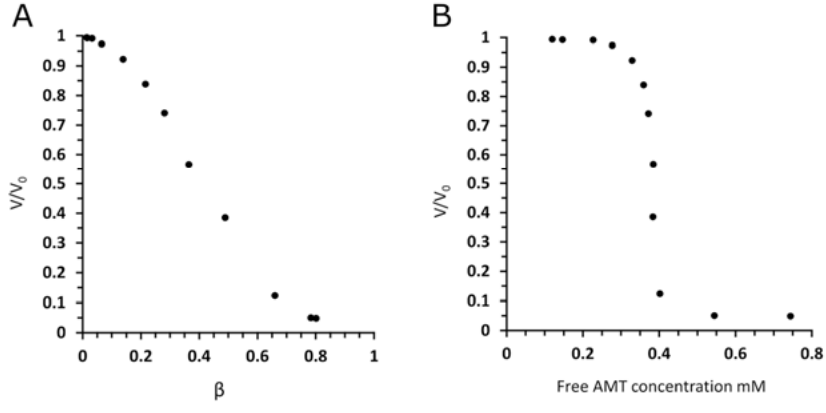

Figure 9. Swelling isotherms for PA macrogels in AMT solution at 10 mM ionic strength.

Loading kinetics at low ionic strength

In this study, a single microgel was positioned in a flow of AMT solution (0.6, 0.8, 1 mM) under controlled conditions. The gel decreased in volume over time as shown in *Figure 10*. Here we have a phase transition from a swollen state to a collapsed one. During the loading process, the gel´s outer layer collapsed and formed a dense shell surrounding a swollen core. The thickness of the shell increased over time at the expense of the swollen part until the whole gel was homogenous and fully collapsed.

The flow rate, AMT concentration and gel size were varied to investigate the mechanism of the loading process. The deswelling time decreased with the increase of the flow rate or the concentration of AMT, while increasing the size of the gel prolonged the deswelling time, as shown in *Figure 11*.

A theoretical model was applied to analyse the deswelling profiles. The drug transport was calculated based on the rate of mass transfer to the gel surface ("stagnant layer diffusion") and inter-diffusion of AMT monomers and sodium ions in the aqueous domains between micelles in the shell. As shown in Paper II, the model predicts well the deswelling profile for the smaller microgels and the higher AMT concentrations, while at a loading concentration 0.6 mM the theoretical curve deviates at the later stages of the loading. The loading rate at this stage was small and a possible explanation to the deviation is that the monomer concentration at the core-shell boundary had time to relax down to the true core-shell equilibrium value. This means that the concentration of the AMT in the inner layer of the shell was smaller than the assigned value in the calculations.

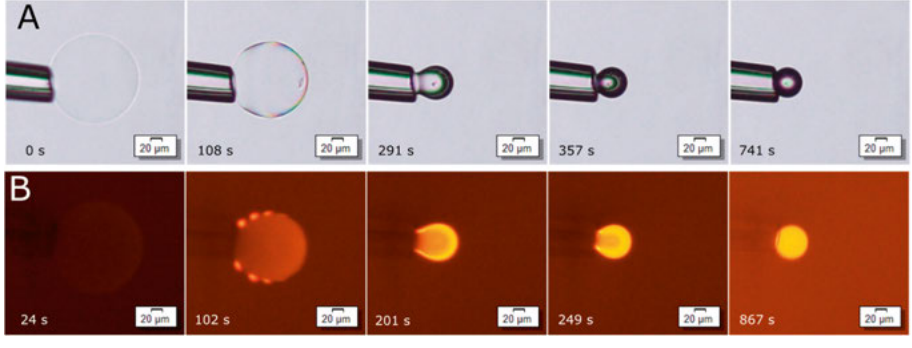

Figure 10. A) Light microscopy images for a single PA microgel during loading with AMT. B) Fluorescence microscopy images for a single PA microgel during loading with AMT. Notice the gel holder to the left of the gel.

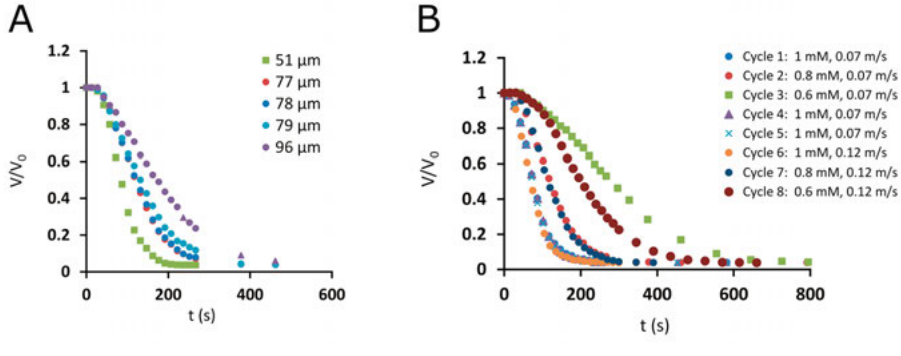

Figure 11. Deswelling kinetics for PA microgel. A) Volume ratio vs time for microgels of different sizes; flow rate: 0.07 m/s and AMT concentration: 0.8 mM. The legend represents the gel radius in 10 mM buffer. B) Volume ratio vs time for a single microgel (radius = 77 µm in 10 mM buffer) in different flow rates and AMT concentrations.

Release kinetics at elevated ionic strength

A single microgel was placed in a flow of AMT solution under controlled conditions. After reaching a homogenous fully collapsed state, the gel was exposed to a buffer solution containing 150 mM NaCl to trigger the release process in a medium of physiological ionic strength, see *Figure 12*. The gel started to release the drug from the outer layer first. Over time the shell grew while the dense core decreased in volume, as more AMT complex dissolved into AMT monomers. The monomers diffused through the shell into the solution outside the gel (sink condition).

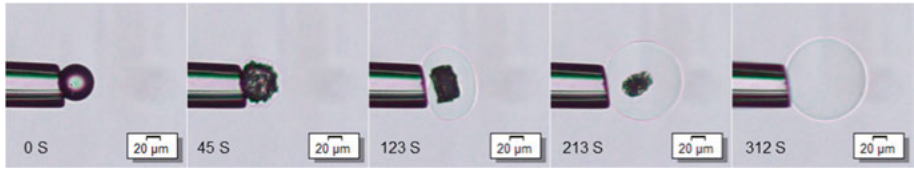

Figure 12. Light microscopy images for a single PA microgel during AMT release at 150 mM NaCl.

The volume changes during release were monitored at specific time intervals. Three gels of different sizes (Table 1) were loaded with AMT and then exposed to elevated ionic strength. Gel 2 was exposed to cycles of loading and release with different loading concentrations and flow rates of the release medium. In each cycle, a loaded gel was exposed to a buffer solution containing 150 mM NaCl until all the AMT released from the gel. After that, the gel was washed with water and loaded with the next AMT concentration. The results showed that increasing the initial size of a gel decreased the swelling rate. However, the loading concentration (1, 0.8, and 0.6 mM) and the flow rate of the release medium did not affect the swelling rate.

The experimental results were compared with theoretical model calculations. The release profiles which are important in drug delivery applications, were successfully described by a theoretical model. *Figure 13A* shows the theoretical curves for the swelling rate. The calculations predict almost quantitatively the effect of the gel size on the swelling rate. *Figure 13B* shows that, by normalizing the time by gel radius in the relaxed state R_{out} to highlight only the influence of the intensive properties, the data in *Figure 13A* collapsed on one master curve. The results suggest that the transport of the drug molecule through the shell is the rate-limiting step for the release and swelling rates. This means that both the aggregation properties of the drug inside the gel and the thickness of the depletion layer (shell), i.e., the distance that the drug monomers need to travel from the core to the gel boundary, are crucial to accurately predict the release profile. In order to correctly describe the evolution

of the shell thickness, the model calculations took into account that the swelling of the shell network is affected by the elastic coupling to the collapsed core network.

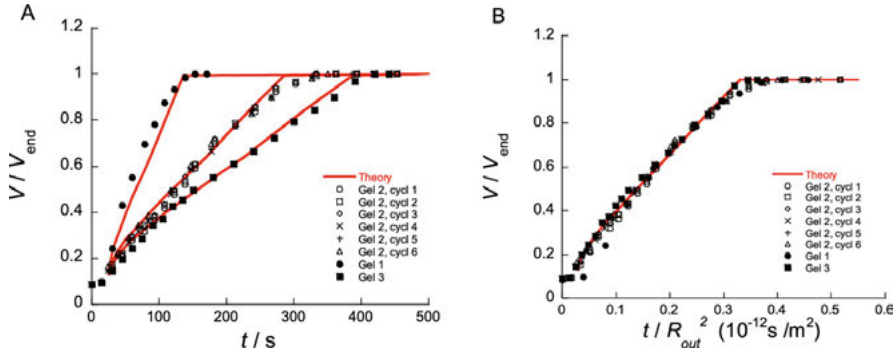

Figure 13. A) Swelling kinetics for PA microgel during AMT release at 150 mM NaCl. Gel radius (r) in water; gel 1= 59 µm, gel 2 = 90 µm, gel gel 3 = 106 µm. Flow rate = 0.07 m/s. Gel 2 experiment performed in 6 cycles with different loading concentrations 1, 0.8, and 0.6 mM, respectively; cycle 1-3 at flow rate 0.07 m/s; cycle 4-6 at 0.12 m/s. V represents the actual microgel volume while V_{end} represents the microgel volume after releasing all AMT. Solid lines represent theoretical swelling curves. B) The time for each curve in (A) was normalized by R_{out}^2, where R_{out} is the radius of the gel in the relaxed reference state.

Table 1. The radius (r) of the microgels in the release experiments.

Gel no	**r (µm)**	**r (µm)**
	No salt	150 mM NaCl
1	59	38
2	90	58
3	106	68

Phase equilibrium in single microgels

We studied the equilibrium properties of one single gel in a limited volume of AMT solution both at 10 mM ionic strength and at 155 mM ionic strength. The amount of AMT was chosen to be enough to load the gel partially with AMT. The aim was to capture the gels at intermediate loading levels to study the stability of the aggregates and the drug distribution inside the gel.

10 mM ionic strength

The swelling isotherm showed that the gel decreased in size with an increase in the binding ratio, see *Figure 14*. At a binding ratio <0.26, the gel was homogenous with no sign of phase separation. The decrease in volume at this stage indicated the presence of drug aggregates inside the gel, since adding the same amount of a simple salt to the solution did not decrease the volume to the same degree. Above 0.26, the phase separation appeared in the gel in the form of dense parts on the outer layer.

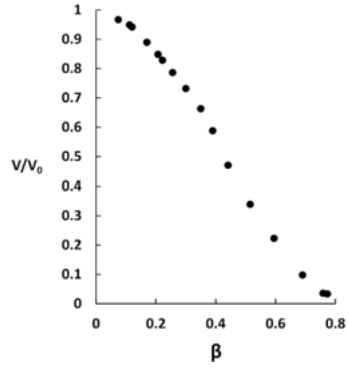

Figure 14. Swelling isotherm for AMT-PA microgel system. V/V_0 was plotted vs binding ratio β.

In the AMT-PA microgel system, the phase separation patterns differ from a core/shell pattern in the surfactant-gel system, see *Figure 15*. At β=0.35, we observed that dense domains on the surface of the gel co-existed with a swollen core. Here the gel still had almost a spherical shape. However, at β=0.6 there was one dense domain in contact with the swollen one. With increasing β, the shape and size of the collapsed part approached the one in the fully collapsed state which means that the collapsed part preferred to be close to the relaxed fully collapsed state. This means that the rearrangement observed was driven by the elastic deformation energy.

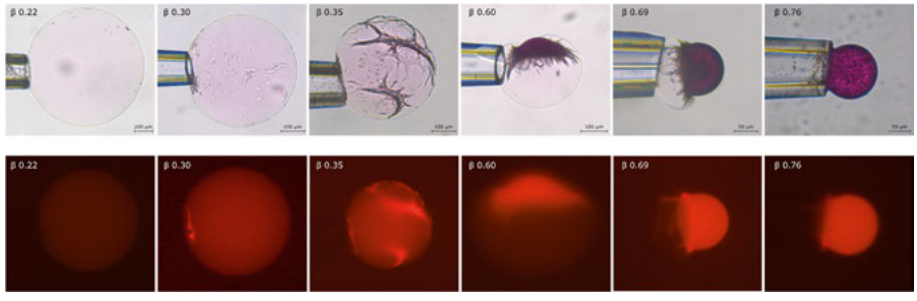

Figure 15. PA microgels equilibrated in a limited amount of AMT solution at 10 mM ionic strength. Each gel represents a separate experiment. Images captured after equilibration by light microscopy (upper row) and fluorescence microscopy (lower row).

To track the drug distribution over time, images were taken at specific intervals. At the beginning, the drug entered the outer layer forming a dense shell surrounding the core. After equilibration, the drug redistributed to form dense domains suspended in the microgel. Interestingly at high binding ratios ($\beta > 0.5$), one big dense domain in contact with a swollen domain appeared, as shown in *Figure 16*. Here the collapsed part dominated over the swollen part and the gel preferred to regain the shape of the fully collapsed gel. The question arises whether the swelling of the swollen part and the AMT concentration in the swollen part increased or not. This was studied in detail by using Raman microscopy technique, see Paper V.

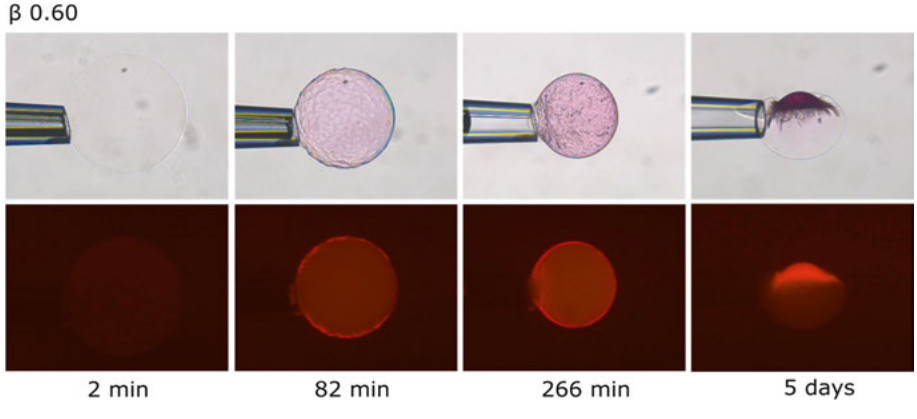

Figure 16. Light and fluorescence microscopy images for one single gel in a limited volume of AMT solution at different time scales. Notice the redistribution of AMT. The final binding ratio β is 0.6.

155 mM ionic strength

We first equilibrated a single gel in 0.7 mM AMT solution (10 mM ionic strength) overnight to reach the fully collapsed state. Then the gel was inserted in a small volume of AMT solution (at 155 mM ionic strength) for 5 hours to

partially release AMT from the gel. Images captured by light microscopy revealed that AMT was released from the outer layer so that a swelled shell formed surrounding the collapsed core, see *Figure 17*.

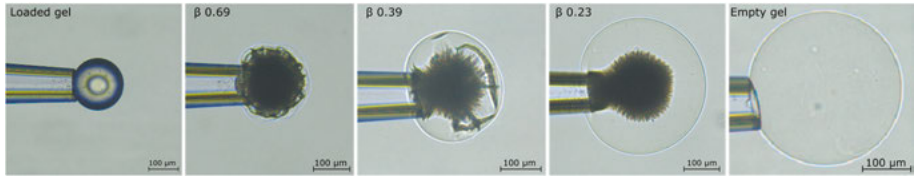

Figure 17. Light microscopy images for different gels equilibrated in a limited volume of AMT solution at 155 mM ionic strength.

In addition, the swelling isotherm showed that the volume of the gel increased with a decrease in the binding ratio and that the swelling trend could be divided into two regimes, see *Figure 18a*. In the first regime (at high β), the shell was thin and the dense part dominated the swollen one. Here the volume of the gel increased moderately with the decrease in the binding ratio to β=0.4. After this point, entering the second regime, the volume increased faster with a decrease in the binding ratio until it reached a homogenous, fully swollen gel state. In the latter regime, the shell dominated over the core in volume. The change in slope of the swelling isotherm when going from the first to the second regime reflects how the presence of the collapsed phase affected the swelling of the swollen phase, and vice versa, due the elastic coupling between them. *Figure 18b* shows the theoretical curve for the swelling isotherm at 155 mM ionic strength. The model assumed that the binding ratio in the core at every instance was similar to the binding ratio in the same fully loaded gel. The model curve lacks a distinct transition point between the two regimes but it describes well the trend of the swelling ratio at low binding ratios and that the swelling increment is largest in the lower binding range where core has the smallest effect on the swelling of the shell.

At this stage, we cannot confirm that the systems in *Figure 17* reached true equilibrium but it is clear that the core-shell phase boundaries remained distinct for extended time periods. This study provides the first experimental evidence that the phase coexistence at intermediate loading levels are stabilized by thermodynamic factors. The results support the theoretical model suggested in Paper II where the release kinetics was tracked indirectly by monitoring the swelling of the gel in controlled conditions. In the model we assumed that phase boundary between core and shell was stabilized by thermodynamic factors during the release process, and that the microgel re-established the osmotic equilibrium quickly at every step of the release process. Thus, the volume of the gel was determined by the amount of AMT remaining in the core.

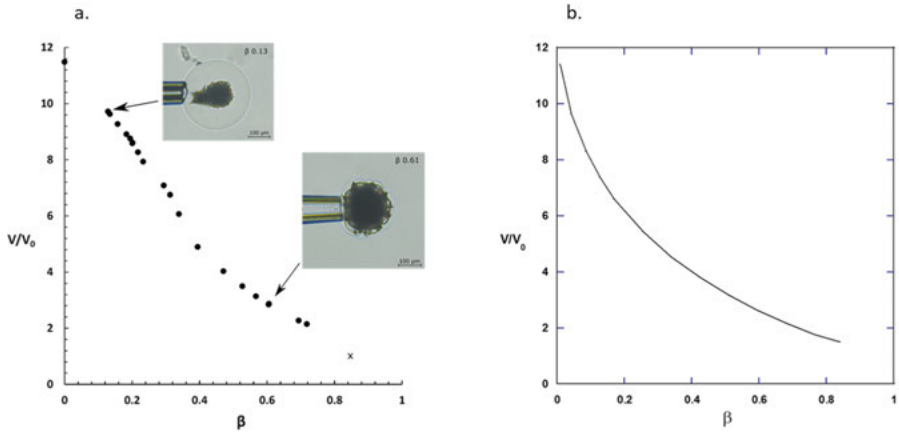

Figure 18. Swelling isotherm for PA microgels equilibrated in a limited volume of AMT solution at 155 mM ionic strength. 5 hours equilibration time. a) Experimental results. The data point (cross) represents a fully collapsed microgel at 10 mM ionic strength. b) Theoretical swelling isotherm.

Binding isotherm at physiological ionic strength

In this study, we investigated phase separation at elevated ionic strength in microgel suspensions by means of binding isotherms. Polyacrylate microgels were equilibrated in solutions with different amounts of AMT at 155 mM ionic strength (pH = 7.4). The results revealed that the binding could be divided into four regimes. The transition points between the regimes are indicated with arrows in the binding isotherm shown in *Figure 19*. At a low AMT concentration, the binding ratio increased slightly with an increase in the AMT concentration until reaching a short plateau which represents the second region. The plateau could be explained by the formation of micelles in the solution outside the gels. This was confirmed by measuring the surface tension for the AMT solution in a buffer system of 155 mM ionic strength. In the third region, the binding increased sharply and the free concentration was almost constant. Microscopy images (at β=0.27) revealed the presence of a phase separation resembling the one at 10 mM ionic strength (see Paper II). The gels collapse one after the other at increasing AMT concentrations until reaching the last region where all the gels are homogenous and fully collapsed. The binding ratio increased slightly to reach values exceeding unity at the end of the investigated concentration range. This was in agreement with theoretical model calculations suggesting that the elevated ionic strength would facilitate the binding ratio over the unity.[77]

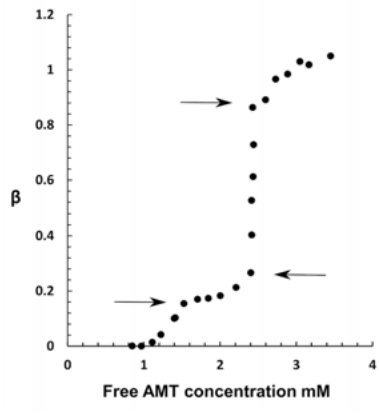

Figure 19. Binding isotherm of AMT-PA microgels at 155 mM ionic strength.

It is interesting to note that the phase separation remained stable at high ionic strength, see *Figure 20*. This was not obvious at the outset, since adding salt is known to dissolve polyelectrolyte complexes. However, the destabilizing effect of the added salt was evidenced by the fact that the critical collapse concentration needed to reach phase separation (CCC) increased from 0.37 mM at 10 mM ionic strength to 2.4 mM at 155 mM ionic strength. The observed equilibrium between collapsed and swollen microgels gives additional support to the idea that the mechanism of drug release at physiological ionic strength can be described as a phase transformation between collapsed and swollen phases as assumed in the release model presented in Paper II.

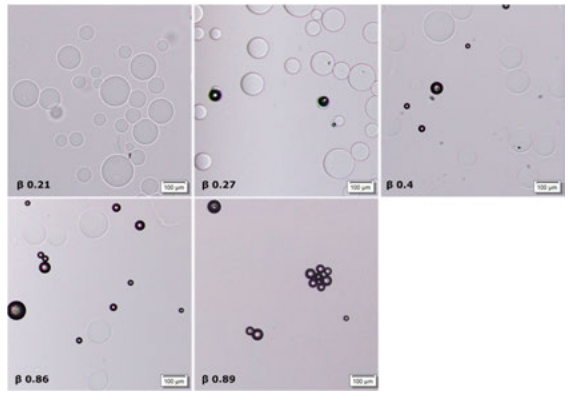

Figure 20. Light microscopy images for PA microgels equilibrated in AMT solution at 155 mM ionic strength. The dark spheres are collapsed PA microgels fully loaded with AMT.

Amphiphilic drugs in DC beads

In Paper I, we investigated the loading and release kinetics of different amphiphilic molecules to/from DC beads. DC Beads are polymer microgels consisting of polyvinyl alcohol attached to poly(2-acrylamido-2-methylpropanesulfonate). These gels possess a negative charge. They can carry a large amount of cationic amphiphilic drugs inside. We studied amitriptyline (AMT), chlorpromazine (CPZ), adiphenine (ADI) and dodecylpyridinium chloride molecules. Micromanipulator-assisted light microscopy was used to inspect the internal morphology of the gels. During the loading process, a single gel was exposed to a flow of amphiphilic drug solution. The results showed that the gel deswelled over time until reaching a homogenous fully collapsed state. The size of the fully collapsed gel was around 10% of the gel before loading for the studied molecules. The deswelling rate was studied by applying different concentrations of each amphiphilic drug. In general, the loading time decreased with an increase in the loading concentrations. Interestingly the variation in the loading rate between different drug molecules (in the studied range) was very small. This can be explained by the large concentration gradient between the loading drug concentration and the critical aggregation concentration inside the gel.

During the release, the gel was exposed to 150 mM ionic strength NaCl solution. The gel swelled gradually over time until reaching a homogenous state, free from the drug. The release starts in the outer layer, forming a swollen shell surrounding a collapsed core. The core consists of drug aggregates which act as a reservoir for the released drug monomers, where the concentration of the monomers in the core equals the critical aggregation concentration CAC.[105] The monomers move through the shell to the outer layer of the gel (sink condition). Here the release rate was not affected by the loading concentration for each studied drug but there were differences between the release profiles of various drugs. The swelling rate increased with increasing critical micelle concentration (CMC).

One major finding in Paper I is an explanation of the mechanism of drug release from DC beads. Previous literature suggested a simple ion-exchange as a primary mechanism to describe the release process.[106-108] In this work, we found that drug aggregation properties inside the gel exerted a significant effect on the release profile. A depletion-layer mechanism was suggested for release, where the drug aggregates in the core´s outer layer dissolve into monomers. The monomers move through the depletion layer, the shell, to the solution outside the gel. This means that the CAC inside the gel can be used to predict the release profile. A drug with a low CMC - and thus CAC (assuming a correlation between CAC and CMC) - has a slower release profile than a drug with a high CMC. This can be explained by the resulting differences in the concentration gradient. A similar mechanism was observed for the release of AMT from PA microgels in Paper II. However, modelling of the release

required more involved calculations taking into account the swelling of the shell during the release. In conclusion, the mechanism of interaction between cationic amphiphilic drugs and oppositely charged microgels provided in Paper I and II can be used to develop novel drug delivery carriers.

Doxorubicin (DOX)-DC beads

The deswelling and swelling rate for DC beads during loading and release of doxorubicin was studied by using micropipette-assisted light microscopy, see *Figure 21*. The hydrophilic and the hydrophobic parts in DOX molecules are not well separated in comparison to other simple cationic amphiphilic drugs, for example amitriptyline. For this reason, we used the surfactant cetylpyridinium chloride (CPC) as a control molecule. It has similar hydrophobic properties to the DOX with a CMC value of 0.9 mM. In general, the volume responsiveness of the gel to DOX is qualitatively the same as in the other studied amphiphilic drugs in Paper I. DC beads decreased in size during the loading process. The drug entered the outermost layer first, forming a collapsed domain. The collapsed part grew as more DOX entered the gel until reaching a fully collapsed gel. The gel at this level contained a large amount of DOX aggregates. This is beneficial in drug delivery applications. After that, exposing the gel to 150 mM NaCl triggered the release process. DOX released from the outermost layer first, forming a swelled shell free from aggregates. It was interesting to observe that the release of DOX was slow and incomplete even after a long exposure time, 6000 s. To understand the incomplete release we need to understand the mechanism behind the release process. The model calculations suggested that the fully loaded gel consists of drug aggregates in equilibrium with free monomers of DOX. The monomer concentration is equivalent to the critical aggregation concentration. This means the concentration of the DOX monomers in a fully collapsed gel is lower than AMT, ADI, and CPZ (see Paper I). The drug released from the outermost layer builds two separated compartments in the gel. The collapsed core full with aggregates is surrounded by a swollen shell free from the aggregate. The core serves as a reservoir for DOX monomers. The monomers move from the core´s outer layer to the bulk via the swelled part. The calculations showed that the concentration gradient between the core and the bulk are an important and rate-limiting step for the release process and not the simple ion-exchange in physiological environments. Due to the low CMC[109] value for DOX and hence CAC, the concentration gradient is lower than for AMT, ADI, CPZ, which affects the release rate. The mechanism highlighted the importance of understanding the aggregation properties in order to predict the release of amphiphilic drugs from microgels.

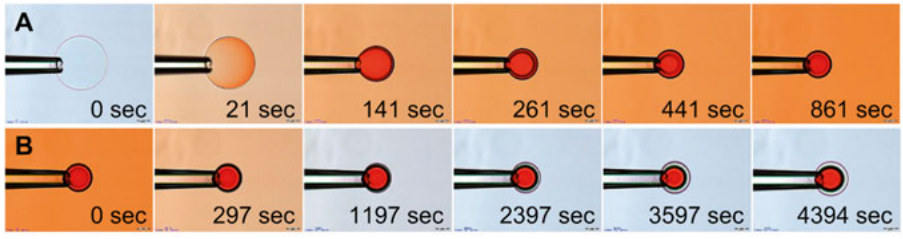

Figure 21. Light microscopy images for DC-beads A) during loading with doxorubicin B) during doxorubicin release.

Aggregation properties inside microgels

Cationic amphiphilic drugs tend to aggregate inside oppositely charged microgels. These self-assembly is beneficial to load substantial amounts of a drug. Polyacrylate microgels, for example, can carry AMT in a concentration of 1.8 M at β=0.85. The aggregation properties affect the loading capacity and the kinetics of loading and release. We found that there is a direct relationship between the critical aggregation concentration (CAC) inside the gel and the release rate, see Paper I. The results highlight the importance of investigating the nature of the drug self-assemblies formed in the microgels. To improve our understanding, we studied the microstructure of polyacrylate microgels loaded with AMT, chlorpromazine (CPZ) and doxepin, respectively by means of the small angle X-ray scattering technique (SAXS). We first equilibrated the microgels in amphiphilic drug solutions of different concentrations. Thereafter, the fully loaded microgels were mounted on a gel holder and scattering curves were collected. The scattering data were analyzed and best fitted by using SasView software. The results revealed that the studied molecules built small ellipsoid micelles inside microgels but no ordered crystalline structures occurred. The scattering curves for AMT, CPZ and doxepin all lack distinct Bragg peaks. They show instead broad correlation peaks. For the samples with binding ratio < 1, this may be explained by the very small aggregation number (see below). However, for the samples with binding ratio > 1, where the aggregation number was higher and the drug concentration inside the microgel was very high, this is remarkable.

In a previously studied C_{12}TAB-gel system at 10 mM ionic strength, the SAXS measurements showed the presence of a cubic liquid crystalline phase[83]. Increasing the ionic strength to 150 mM dissolved the order structure. In addition, Ashbaugh and Lindman[110] studied the effect of the micelle surface charge on the scattering curves in a similar system. The non-ionic surfactant octaethylene glycol monododecyl ether ($C_{12}E_8$) was added in different proportions to the complex to form mixed micelles with the cationic surfactant in the

gel. They found that increasing the proportion of non-ionic surfactant in micelles shifted the cubic peaks to lower q values. Further increase in the $C_{12}E_8$ content caused disappearance of the distinct peaks to form a broad correlation peak instead. This showed that decreasing the surface charge of the micelles "melted" the liquid crystalline phase into a disordered micellar phase.

Returning to our work, the ionization degree of AMT, CPZ and doxepin are sensitive to the pH of the medium. At pH 7.4 there is a small percent of uncharged species in the liquid solution.[46] However, with increasing drug concentration in the solution there is a hydrophobic driving force to continue incorporating drug even beyond the point where the binding ratio is larger than unity. The systems can accomplish this without excessive "overcharging" of the gels by recruiting preferentially uncharged drug molecules from the solution. It is possible that the lack of liquid crystalline order, even in the most highly concentrated microgels, can be explained by the presence of uncharged species in the micelles, weakening the electrostatic interactions in the complexes.

In the AMT-PA microgels system, we equilibrated a suspension of microgels in 1-20 mM AMT solution at 10 mM ionic strength. The scattering data at 1 mM solution showed a broad correlation peak at scattering vector $q \approx 0.3$. Increasing the concentration in the solution caused a shift of the maximum to lower q, see *Figure 22*. Above 10 mM, the curve resembled the ones observed previously by Efthymiou et al.[46] in the AMT-water system well above CMC. The curves are typical for a system of micelles interacting with each other. In such systems, the scattering is dominated by the form factor at low concentrations but strongly influenced by the structure factor at higher concentrations, supressing the scattering at low q. Thus, since there are large concentration effects on the scattering curves it is important to be able to determine the concentration of the drug inside a microgel. Such measurements impose a challenge in a microscale experiment. However, in Paper IV, we succeeded in measuring the concentration of the drug inside the microgels by building a microscopy cell specially designed to equilibrate one single microgel inside a specific concentration of the drug. After equilibration, the gel became homogenous and fully collapsed. We used a μDISS profiler to determine the amount of the drug inside the gel as described above, in combination with determination of gel volumes from microscopy images. The results revealed that the concentration of AMT inside the gel increased with increasing loading concentrations in the range of 1-20 mM of AMT solution. It is noteworthy that the gel at 1 mM reached a fully collapsed state. This means that loading continued after reaching non-cooperative binding (see *Figure 7*). The scattering curves showed sensitivity to the concentration of the drug inside the gels. As the concentration in the gel increased, the correlation peak shifted to lower q and the influence of the structure factor decreased. This is contrary to the AMT scattering curves in water, where the maximum of the scattering curves shifted to higher q and the influence of the structure factor increased with increasing

concentration.[46] This can be explained by the ratio of the non-ionic to ionic species in the micelles. As the non-ionic proportion inside the micelles rises, the aggregation number grows, and thus in a closely packed system the centre-centre distance between micelles increases. This results in a shift in the correlation peaks to lower q.

The shape of the scattering curves could be fitted with a scattering model for ellipsoidal micelles. We used a two-compartment (core/shell) model in which the micelle consists of a core and shell with different electron density. The polyion-dressed hydrophilic head groups of an amphiphilic drug comprise the electron rich shell while the hydrophobic moieties represent the core. The main parameters for this model are the polar axis, equatorial axis and shell thickness. The ratio of polar to equatorial semi-axis (r_{polar}/r_{equ}) describes the ellipticity of the micelles. The r_{polar}/r_{equ} ratio less than 1 indicates the presence of oblate ellipsoid micelles while the r_{polar}/r_{equ} ratio higher than 1 indicates the presence of prolate ellipsoid micelles. We used a core-shell ellipsoid model combined with Hayter-Penfold RMSA structure factor to determine the shape of the aggregates formed by AMT, CPZ and doxepin in PA microgels. The structure factor was necessary to take into account the effect of the interactions between adjacent micelles.

In the AMT-PA microgels system, fitting the scattering curves showed that the micelles have oblate ellipsoid form with a small aggregation number. The micelles became more elongated as the binding ratio increased. The polar-to-equatorial ratio decreased with an increase in AMT binding ratio from 0.9 at β 0.85 to 0.5 at β 2.1.

At β 0.85 the aggregation number inside the microgel was 11. The aggregation number was increased with an increase in the equilibrium concentration to reach 42 at β 2.1. The micelles grew mainly by extending the length of the equatorial axis. The aggregation number is comparable to the ones reported for AMT in concentrated aqueous solutions.[46] Interesting to point out is that at β 2.1, the model fitted the experimental scattering curve with a very small shell thickness. This means that the difference in the electron density between the core and the shell was small. Actually, it was possible to fit the curve by using a homogenous ellipsoid model resembling the one previously used in AMT-water system. This indicates the influence of the increase in the non-ionic species in the complex.

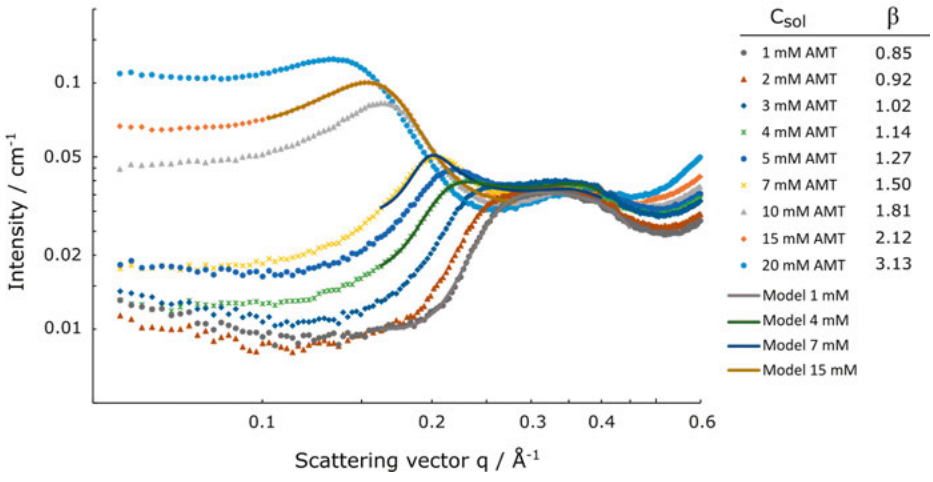

Figure 22. SAXS scattering curves for AMT-PA microgels. C_{sol} represents drug concentration in a solution in equilibrium with the microgel. β represents the binding ratio. Solid lines represent the fitting curves performed by SasView.

The effect of ionic strength on the aggregation properties was studied by equilibrating microgels in AMT solution at low and high ionic strength. The binding ratio was set to 0.84 and 0.89 in 10 mM and 155 mM ionic strength, respectively. *Figure 23* showed that at elevated ionic strength the scattering curve was broader than at 10 mM ionic strength. The curve resembles the ones recorded at 3 mM AMT solution, see *Figure 22*. Also the curve for AMT-PA at 10 mM ionic strength, resembles the one at 1 mM equilibrium concentration. There was similarity between the curves towards high q, where the scattering pattern is dominated by the form factor. This means that the aggregation number did not changed much. However, elevating the ionic strength decreased the influence of the structure factor. This means that the interaction between micelles decreased at high ionic strength.

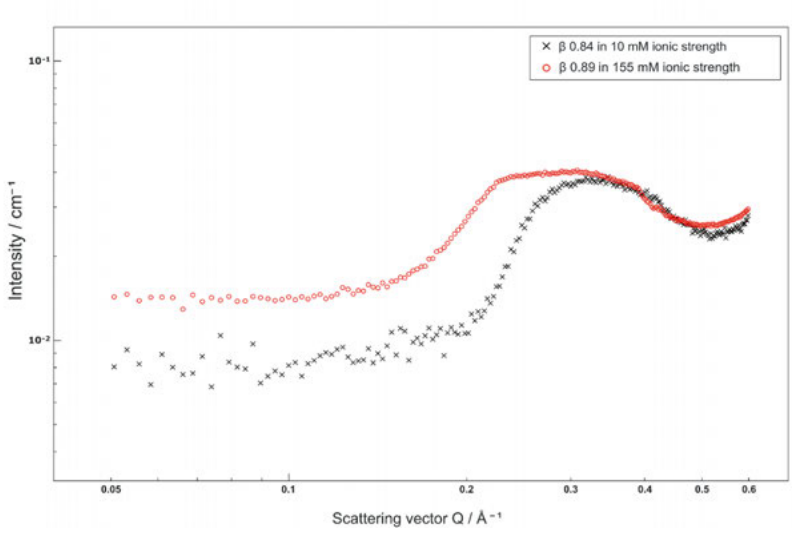

Figure 23. SAXS curves for AMT- PA system at 10 mM and 155 mM ionic strength.

The scattering curves for chlorpromazine-PA microgels at 10 mM ionic strength also indicated a strong correlation between micelles. The maximum scattering intensity increased when increasing the equilibrium concentration from 0.25 mM to 0.5 mM, but was followed by a drop in the intensity when the concentration was further increased to 1 mM, 2 mM and 3 mM, as shown in *Figure 24*.

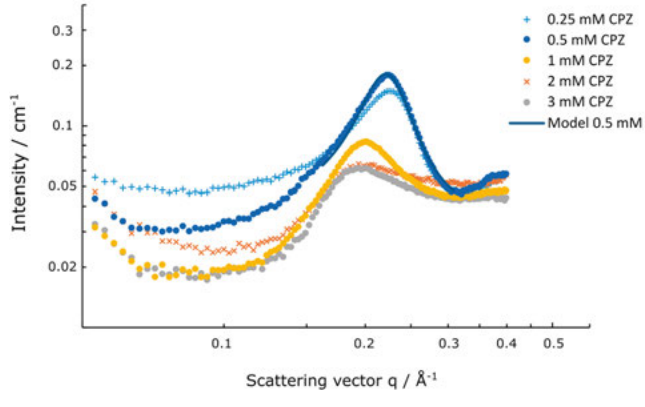

Figure 24. SAXS curves for CPZ-PA microgels system at 10 mM ionic strength. The legend represents drug concentration in a solution in equilibrium with the microgel.

The latter effect was unexpected but could be explained by microscopy images for a single microgel equilibrated in solutions with 0.25 - 3 mM CPZ, revealing that CPZ precipitated on the surface of the gel for concentrations ≥ 1 mM, see *Figure 25*. Thus it is likely that, for those samples, the concentration in the

gels was lower than expected. At 0.5 mM CPZ, the experimental curve was best fitted by using a model with a core-shell ellipsoid form factor and Hayter RMSA structure factor. The result showed that CPZ-microgels complex form oblate shape aggregates with aggregation number 23.

Figure 25. Microscopy images for CPZ-PA microgel system at 10 mM ionic strength.

The scattering curves for the doxepin-PA microgels system at 10 mM ionic strength were rather insensitive to variations in the equilibrium concentration. As shown in *Figure 26*, the pattern of the curves remained almost the same in the studied range between 2 mM and 5 mM equilibrium concentration. The binding ratio inside the gel revealed that the amount of doxepin inside the gel remained the same after increasing the equilibrium concentration in the studied range. This explains the similarity of the scattering curves. A theoretical model based on a core-shell ellipsoid form factor combined with a Hayter RMSA structure factor was fitted on the scattering data for doxepin-PA microgels complex at 5 mM doxepin solution. The results revealed that the aggregates form small oblate ellipsoid micelles with aggregation number 11.

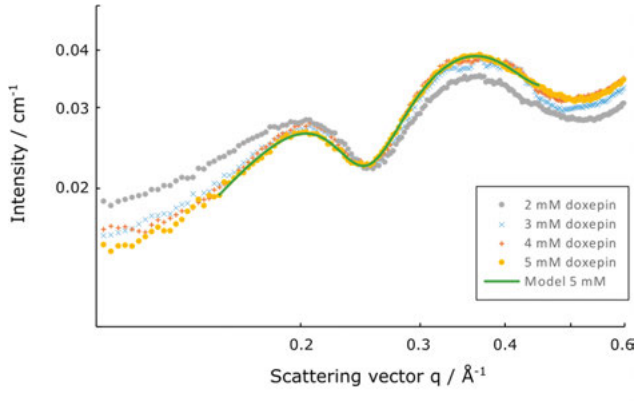

Figure 26. SAXS curves for doxepin-PA microgels system at 10 mM ionic strength. The legend represents the equilibrium concentration.

In conclusion, we combined different experimental techniques to study the aggregation properties inside microgels. These properties are very important in understanding the drug-microgels interactions and thus predict loading and release profiles.

Composition of the swollen phase

In Paper II, we noticed that microgels at a high binding ratios, redistributed from a core/shell pattern to an asymmetric pattern. Furthermore, the intensity of the fluorescent probe in the swelled part was lower than in a gel with a binding ratio just below the phase separation limit. This indicated that the AMT concentration in the swollen part could actually decrease upon phase separation, a behaviour that would resemble precipitation in a supersaturated solution. However, in gels this could be caused by elastic effects rather than by interfacial tension. To investigate this we used, in Paper V, the Raman microscopy technique to track the changes in the composition of different parts of homogeneous and phase separated microgels. A new microscopy cell design was used in this work to be able to perform Raman measurements. After equilibration of a single polyacrylate microgel in a small volume of AMT solution, the gel tended to partially collapse, forming a dense phase in contact with a swollen phase. A set of microgels with different binding ratios could be created by controlling the initial concentration of the drug in the solution, the volume of the solution and the size of the gel. In gel 1, the binding ratio was 0.25. The gel volume decreased upon loading of the drug but the gel remained homogenous with no sign of phase separation, see *Figure 27*. This was in agreement with the results in Paper III, where phase separation of a single PA gel in AMT solution was first noticed at β=0.26. It is worth mentioning that in a suspension of PA microgels equilibrated in AMT solution, phase separation occurred at β=0.22, see Paper II.

As shown in *Figure 27*, at a binding ratio of 0.34, gel 6 consisted of collapsed domains in contact with swollen ones. The gel was deformed but still retained a globular shape. At $\beta > 0.5$, the separation into a collapsed and a swollen phase was more distinct. The gel deformed heavily on the side of the collapsed part while the swelled one appeared to strive to maintain the shape before phase separation.

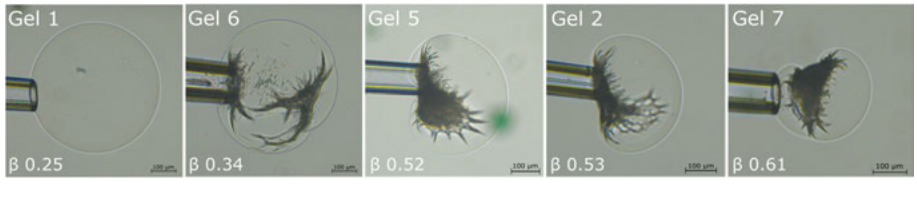

Figure 27. Light microscopy images for PA microgels equilibrated in a limited volume of AMT solution. Each image represents a separate experiment.

Raman spectra (see *Figure 28*) showed that the concentration of AMT in the swollen part of a gel with a binding ratio 0.53 was lower than in a loaded gel just before phase separation (binding ratio 0.25). This means that the concentration needed to start collapsing a swelled gel is higher than the Maxwell

point, which is the concentration at which swollen homogeneous and collapsed homogeneous gel states have the same free energy. This can be explained by the presence of elastic forces in the polymer networks that act as an energy barrier hindering the phase separation to occur.[78, 85] Once phase separation occurs, the gel network relaxes with an increase in the binding ratio. With that the chemical potential of the drug, and therefore also the concentration of drug monomers in the swollen phase decreases. This explains also the hysteresis in the equilibrium concentration needed to collapse a swelled gel during loading and to swell a collapsed gel during release.

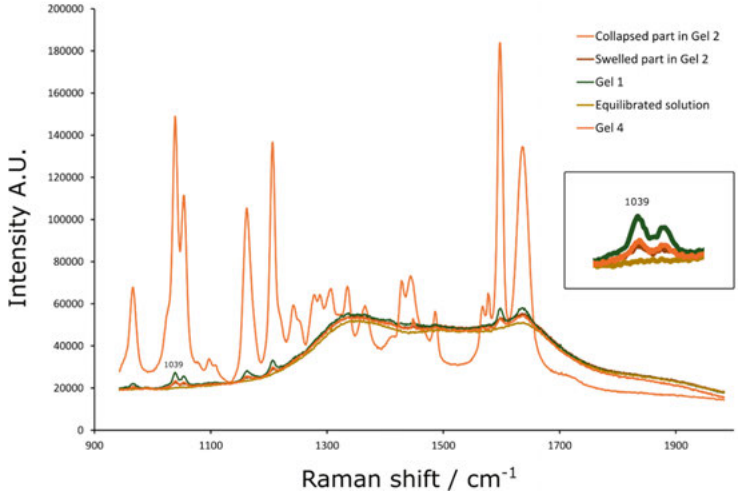

Figure 28. Raman spectra for different parts in a single microgel equilibrated in a small volume of AMT solution. The equilibrium solution, in legend, represents the AMT solution in equilibrium with gel 2. Gel 1; β_{gel1} 0.25, homogenous gel with no phase separation. Gel 2; β_{gel2} 0.53, phase co-existence. Gel 4; β 0.22, homogenous gel with no phase separation, equilibrated in 2 gels system.

We further studied this effect by performing a separate experiment where we inserted two microgels in a limited volume of AMT solution, sufficient to load one gel with a binding ratio 0.55 or both with 0.275. Initially, both gels decreased in volume, indicating that micelles formed in them. However, after a few days, one of them further decreased in volume at the same time as a collapsed phase appeared in it, while the other gel increased slightly in volume, see *Figure 29*. This means that AMT redistributed between the gels. According to the above results for single microgels, the nucleation of the collapsed phase requires a minimum binding ratio of ca. 0.26, which is just below the binding ratio in each gel if AMT would have distributed uniformly between them. Thus, in principle both gels could have been in the phase separated state. However, the observed non-uniform distribution with the collapsed phase in

one of the gels is expected to be consistent with the lowest elastic deformation energy.

It is interesting to note that the binding ratio of gel 4 decreased to 0.22, as obtained from comparison with the swelling isotherm for a single PA microgel in Paper III. This is the same value as the minimum binding ratio required for collapsed microgels to coexist with swollen microgels in suspensions of PA microgels in AMT solutions (see *Figure 8*). This means that the average deformation energy per microgel in a suspension of collapsed and swollen microgels is lower than in a phase separated single microgel.

Understanding the effect of elastic forces on the loading and release processes enhances understanding of the mechanism of interactions and thus improves theoretical models, which can predict release profiles in such delivery systems with high accuracy.

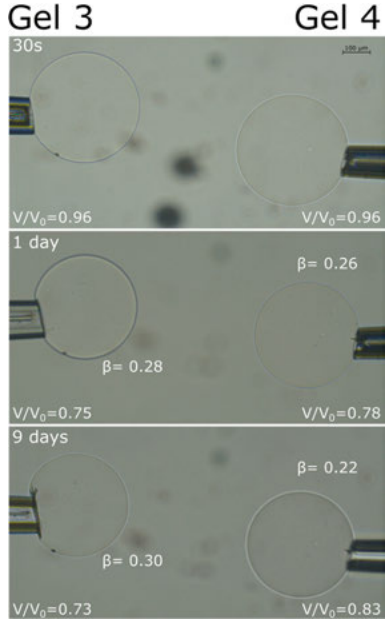

Figure 29. Microscopy images of two PA microgels in a limited volume AMT solution. V/V_0 represents the volume ratio where V is the actual volume and V_0 is the initial volume in 10 mM phosphate buffer before adding AMT. The binding ratio β is derived from the swelling isotherm in Paper III.

Conclusions

The focus of this thesis was on understanding the interaction between cationic amphiphilic drugs and oppositely charged microgels. The findings are valuable to the design of a novel drug delivery system based on loading a large amount of amphiphilic drug inside microgels with the possibility to control the release. We successfully used different experimental techniques to obtain thermodynamic, compositional and microstructural information that are essential to understand the mechanism of the loading and release.

A depletion-layer mechanism was suggested for the release process. During the release, a swelled shell formed, free of aggregate, surrounding a collapsed core. The self-assembling properties of the amphiphilic drugs inside the core have a direct influence on the release profile. The calculations suggest that the transport of the drug through the shell is the rate-determining step. Here the stability of the aggregates in the core and the concentration gradient for drug monomers between the core and the gel´s outer layer play a major role. In addition, the distance from the core to the shell that the monomers travel should be taken into account, especially for highly responsive microgels.

We succeeded in designing a new microscopy cell suitable for microscale experiments to investigate the stability of the phase coexistence. For AMT-PA microgel system, we concluded that the phase separation could be stabilized by thermodynamic factors. In addition, equilibrating a suspension of PA microgels with AMT at a physiologically relevant ionic strength reveals a bimodal distribution of the drug where the drug prefers to aggregate in one gel at a time. If there is sufficient amount of drug molecules, the gels collapse one after the other until all the gels are fully collapsed. The findings indicate that the sharp boundary between the collapsed and the swelled part during the release process, in Paper II, is influenced by thermodynamic interactions and not a result of slow dynamics.

The SAXS scattering curves for the AMT, CPZ and doxepin in PA microgels showed no ordered crystalline structures despite the drug being very concentrated inside the gel. The drug aggregates formed small ellipsoidal micelles. In AMT-PA microgels complex, the aggregation number increased with an increase in the concentration of the drug inside the gel. We concluded that the presence of nonionic species, which form mixed micelles together

with ionic species, influences the aggregation properties. Here further investigations are needed to quantify the ratio of ionic to nonionic species.

We compared the intensity of Raman spectra for AMT in PA microgel with different loading levels to investigate the effect of the elastic coupling between the swollen and collapsed phases. The results revealed that the cost of deformation acts as a hindrance to phase separation at the Maxwell point. But once phase separation occurs, the concentration of the drug needed to stabilize the phase coexistence decreases with an increase in the loading level inside the gel. This information is valuable to understanding the hysteresis between the swelling and collapse transitions, which is important for improving the prediction of release profiles.

Future perspective

The information obtained from this thesis can be used as a foundation to study more complex amphiphilic biomacromolecules in microgels systems.

In this thesis, we investigated the effect of ionic strength on the interactions between amphiphilic drugs and microgels carrier systems. We recommend expanding these studies by using different trigger factors such as glucose, pH and temperature. Furthermore, it would be interesting to investigate how the addition of albumin to the solution as a competitor to the microgels for binding of drug molecules would affect the drug release.

A time-resolved fluorescence quenching technique can be used to study the aggregation number of drug aggregates inside microgels. This technique offers complementary information to the results obtained from SAXS. Finally, we suggest expanding Raman microscopy studies to investigate the ratio of ionic to non-ionic species of drug aggregates inside microgels.

Acknowledgements

My doctoral studies were carried out in the *Department of Pharmacy* and the *Department of Medicinal Chemistry*. Belonging to two departments during my PhD period provided a unique opportunity to meet creative colleagues with different expertise and share knowledge in two departments full of highly motivated people.
My project is part of the drug delivery research forum *SweDeliver*. I am grateful to *SweDeliver* for financial support and most importantly for providing such a creative research environment that helped me articulate my knowledge.

Above all, my heartfelt thanks go to my supervisor *Per Hansson*. I am most grateful for all the discussions and assistance, where your knowledge in the field shone and truly inspired me. For the deepening of my scientific and personal knowledge. I am really lucky to have you as a supervisor and I owe you my deepest gratitude.
My co-supervisor *Magnus Bergström*, thank you for helping me to find answers for many fundamental questions regarding self-assembly.

I want to thank my co-authors *Emelie Ahnfelt*, *Jonas Gernandt*, *Erik Sjögren*, *Hans Lennernäs* and *Tomas Edvinsson* for our productive collaboration.

I wish to thank *Susanna Abrahmsen-Alami* and *Andreas Hugerth* for our innovative and productive discussions. Thanks to my mentor *Sofia Lindqvist* for the professional advice.
Christel Bergström thank you for all help and support, your energy knows no boundaries.
Thank you *Adrian Rennie* and *Johan Gråsjö* for sharing your expertise in X-ray scattering technique.

The work with the Pharmaceutical Physical Chemistry group gave much joy, thanks *Marcus*, *Julia*, *Vahid*, *Ellen*, *Sana*, *Agnes* and *Victor* for all help and support. I felt truly lucky with our collaboration.
Randi, *Lina*, *Claes* and *Lotta* your help at the beginning of my project is deeply appreciated.

To the drug delivery seminar´s group *Katarina Edward*, *Lars Gedda*, *Philipp*, *Luis*, *Oliver* and *Fredrik* thank you for the solid scientific discussions, you inspired my knowledge in the field.

Pongsters *Irès*, *Sohan*, *Aleksei*, *Shakhawath*, *Rosita* and *Marilena*. I really spent a fun time with you. A lot of laughter and relaxing time, every Monday night playing Innebandy and our pong tournaments, I will miss these for sure.

To my family: *Farah* my sweetheart, thanks for your help during my studies, my success means nothing without you. *Faisal, Dalia and Najib*, your energy always inspired me. My parents *Atyaf & Mohammed Najib*, it is hard to find words to describe my gratitude, without you all this progress would not have happened. I wish to thank *Alhan, Dina, Hani, Hasan* and *Haya*, for the truly love and encouragement throughout my studies.

Yassir Al-Tikriti
Uppsala, april 2022

References

1. Park, K., Controlled drug delivery systems: Past forward and future back. *J. Controlled Release* **2014,** *190*, 3-8.
2. Lin, C.-C.; Metters, A. T., Hydrogels in controlled release formulations: Network design and mathematical modeling. *Adv. Drug Delivery Rev.* **2006,** *58*, 1379–1408.
3. Narayanaswamy, R.; Torchilin, V. P., Hydrogels and Their Applications in Targeted Drug Delivery. *Molecules (Basel, Switzerland)* **2019,** *24* (3), 603.
4. Mikhail, A. S.; Mauda-Havakuk, M.; Negussie, A. H.; Hong, N.; Hawken, N. M.; Carlson, C. J.; Owen, J. W.; Franco-Mahecha, O.; Wakim, P. G.; Lewis, A. L.; Pritchard, W. F.; Karanian, J. W.; Wood, B. J., Evaluation of immune-modulating drugs for use in drug-eluting microsphere transarterial embolization. *International Journal of Pharmaceutics* **2022,** *616*, 121466.
5. Malmsten, M.; Bysell, H.; Hansson, P., Biomacromolecules in microgels - opportunities and challanges for drug delivery. *Curr. Opin. Colloid Interface Sci.* **2010,** *15*, 435-444.
6. Dosio, F.; Arpicco, S.; Stella, B.; Fattal, E., Hyaluronic acid for anticancer drug and nucleic acid delivery. *Adv. Drug Delivery Rev.* **2016,** *97*, 204–236.
7. Peppas, N. A.; Buresa, P.; Leobandunga, W.; Ichikawa, H., Hydrogels in pharmaceutical formulations. *European Journal of Pharmaceutics and Biopharmaceutics* **2000,** *50*, 27-46.
8. Censi, R.; Di Martino, P.; Vermonden, T.; Hennink, W. E., Hydrogels for protein delivery in tissue engineering. *J. Controlled Release* **2012,** *161* (2), 680-692.
9. Wechsler, M. E.; Stephenson, R. E.; Murphy, A. C.; Oldenkamp, H. F.; Singh, A.; Peppas, N. A., Engineered microscale hydrogels for drug delivery, cell therapy, and sequencing. *Biomed. Microdevices* **2019,** *21* (2), 31-31.
10. Yoshida, R.; Sakai, K.; Okano, T.; Sakurai, Y., Pulsatile drug delivery systems using hydrogels. *Adv. Drug Del. Rev.* **1993,** *11*, 85-108.
11. Dadsetan, M.; Liu, Z.; Pumberger, M.; Giraldo, C. V.; Ruesink, T.; Lu, L.; Yaszemski, M. J., A stimuli-responsive hydrogel for doxorubicin delivery. *Biomaterials* **2010,** *31* (31), 8051-8062.
12. Sjöberg, H.; Persson, S.; Caram-Lelham, N., How interactions between drugs and agarose-carrageenan hydrogels influence the simultaneous transport of drugs. *J. Controlled Release* **1999,** *59* (3), 391-400.
13. Vinogradov, S. V., Colloidal microgels in drug delivery applications. *Curr. Pharm. Des.* **2006,** *12*, 4703-4712.
14. Liang, J.; Xiao, X.; Chou, T.-M.; Libera, M., Counterion Exchange in Peptide-Complexed Core–Shell Microgels. *Langmuir* **2019,** *35* (29), 9521-9528.
15. Hoare, T. R.; Kohane, D. S., Hydrogels in drug delivery: Progress and challenges *Polymer* **2008,** *49*, 1993–2007.

16. Ende, M. T.; Peppas, N. A., Transport of ionizable drugs and proteins in cross-linked poly(acrylic acid) and poly(acrylic acid-co-2-hydroxyethyl methacrylate) hydrogels. II. Diffusion and release studies. *J. Controlled Release* **1997,** *48* (1), 47-56.
17. Bysell, H.; Hansson, P.; Malmsten, M., Transport of poly-L-lysine into oppositely charged poly(acrylic acid) microgels and its effect on gel deswelling. *J. Colloid Int. Sci.* **2008,** *323*, 60-69.
18. Bysell, H.; Hansson, P.; Malmsten, M., Effect of charge density on the interaction between cationic peptides and oppositely charged microgels. *J. Phys. Chem. B* **2010,** *114*, 7207-7215.
19. Bysell, H.; Schmidtchen, A.; Malmsten, M., Binding and Release of Consensus Peptides by Poly(acrylic acid) Microgels. *Biomacromolecules* **2009,** *10* (8), 2162-2168.
20. Hansson, P.; Bysell, H.; Månsson, R.; Malmsten, M., Peptide-microgel interaction in the strong coupling regime. *J. Phys. Chem. B* **2012,** *116*, 10964-10975.
21. Eichenbaum, G. M.; Kiser, P. F.; Simon, S. A.; Needham, D., pH and ion-triggered volume response of anionic hydrogel microspheres. *Macromolecules* **1998,** *31*, 5084-5093.
22. Saunders, B. R.; Crowther, H. M.; Vincent, B., Poly[(methyl methacrylate)-co-(methacrylic acid)] Microgel Particles: Swelling Control Using pH, Cononsolvency, and Osmotic Deswelling. *Macromolecules* **1997,** *30* (3), 482-487.
23. Varela, M.; Real, M. I.; Burrel, M.; Forner, A.; Sala, M.; Brunet, M.; Ayuso, C.; Castells, L.; Montañá, X.; Llovet, J. M.; Bruix, J., Chemoembolization of hepatocellular carcinoma with drug eluting beads: Efficacy and doxorubicin pharmacokinetics. *Journal of Hepatology* **2007,** *46* (3), 474-481.
24. Jordan, O.; Denys, A.; De Baere, T.; Boulens, N.; Doelker, E., Comparative Study of Chemoembolization Loadable Beads: In vitro Drug Release and Physical Properties of DC Bead and Hepasphere Loaded with Doxorubicin and Irinotecan. *J. Vasc. Interv. Radiol.* **2010,** *21* (7), 1084-1090.
25. Ahnfelt, E.; Sjögren, E.; Hansson, P.; Lennernäs, H., In Vitro Release Mechanisms of Doxorubicin From a Clinical Bead Drug-Delivery System. *J. Pharm. Sci.* **2016,** *105* (11), 3387-3398.
26. Lewis, A. L.; Gonzalez, M. V.; Lloyd, A. W.; Hall, B.; Tang, Y.; Willis, S. L.; Leppard, S. W.; Wolfenden, L. C.; Palmer, R. R.; Stratford, P. W., DC Bead: In Vitro Characterization of a Drug-delivery Device for Transarterial Chemoembolization. *J. Vasc. Interv. Radiol.* **2006,** *17* (2, Part 1), 335-342.
27. Lewis, A. L.; Holden, R. R., DC Bead embolic drug-eluting bead: Clinical applications in the locoregional treatment of tumors. *Expert Opin. Drug Delivery* **2011,** *8* (2), 153-169.
28. Pelton, R., Temperature-sensitive aqueous microgels. *Adv Colloid Interface Sci* **2000,** *85* (1), 1-33.
29. Lengyel, M.; Kállai-Szabó, N.; Antal, V.; Laki, J. A.; Antal, I., Microparticles, Microspheres, and Microcapsules for Advanced Drug Delivery. *Sci. Pharm.* **2019,** *87* (3).
30. Eichenbaum, G. M.; Kiser, P. F.; Dobrynin, A. V.; Simon, S. A.; Needham, D., Investigation of the swelling response and loading of ionic microgels with drugs and proteins: The dependence on cross-link density. *Macromolecules* **1999,** *32*, 4867-4878.
31. Johansson, C.; Hansson, P.; Malmsten, M., Interaction between lysozyme and poly(acrylic acid) microgels. *J. Coll. Int. Sci.* **2007,** *316*, 350-359.

32. Johansson, C.; Hansson, P.; Malmsten, M., Mechanism of lysozyme uptake in poly(acrylic acid) microgels. *J. Phys. Chem. B* **2009,** *113*, 6183-6193.
33. Månsson, R.; Bysell, H.; Hansson, P.; Schmitdchen, A.; Malmsten, M., Effect of peptide secondary structure on the interaction with oppositely charged microgels. *Biomacromolecules* **2011,** *12*, 419-424.
34. Eichenbaum, G. M.; Kiser, P. F.; Shah, D.; Simon, S. A.; Needham, D., Investigation of the swelling response and drug loading of ionic microgels: The dependence on functional group composition. *Macromolecules* **1999,** *32*, 8996-9006.
35. Thalberg, K.; Lindman, B., Gel formation in aqueous systems of a polyanion and an oppositely charged surfactant. *Langmuir* **1991,** *7*, 277-83.
36. Evans, F.; Wennerström, H., *The Colloidal Domain: where Physics, Chemistry, Biology, and Technology Meet*. VCH Publishers: New York, 1994.
37. Tanaka, T., Collapse of gels and the critical endpoint. *Phys. Rev. Lett.* **1978,** *40* (12), 820-823.
38. Tanaka, T.; Sato, E.; Hirokawa, Y.; Hirotsu, S.; Peetermans, J., Critical kinetics of volume phase transition of gels. *Phys Rev Lett* **1985,** *55* (22), 2455-2458.
39. Johansson, L.; Skantze, U.; Loefroth, J. E., Diffusion and interaction in gels and solutions. 2. Experimental results on the obstruction effect. *Macromolecules* **1991,** *24* (22), 6019-6023.
40. Johansson, L.; Elvingson, C.; Loefroth, J. E., Diffusion and interaction in gels and solutions. 3. Theoretical results on the obstruction effect. *Macromolecules* **1991,** *24* (22), 6024-6029.
41. Schneider, S.; Linse, P., Monte Carlo Simulation of Defect-Free Cross-Linked Polyelectrolyte Gels. *The Journal of Physical Chemistry B* **2003,** *107* (32), 8030-8040.
42. Lewis, A. L.; Gonzalez, M. V.; Lloyd, A. W.; Hall, B.; Tang, Y.; Willis, S. L.; Leppard, S. W.; Wolfenden, L. C.; Palmer, R. R.; Stratford, P. W., DC Bead: In Vitro Characterization of a Drug-delivery Device for Transarterial Chemoembolization. *Journal of Vascular and Interventional Radiology* **2006,** *17* (2, Part 1), 335-342.
43. Dosio, F.; Arpicco, S.; Stella, B.; Fattal, E., Hyaluronic acid for anticancer drug and nucleic acid delivery. *Adv Drug Deliv Rev* **2016,** *97*, 204-36.
44. Attwood, D., The mode of association of amphiphilic drugs in aqueous solution. *Adv. Colloid Interface Sci.* **1995,** *55*, 271-303.
45. Schreier, S.; Malheiros, S. V. P.; de Paula, E., Surface active drugs: self-association and interaction with membranes and surfactants. Physicochemical and biological aspects. *Biochim. Biophys. Acta, Biomembr.* **2000,** *1508* (1), 210-234.
46. Efthymiou, C.; Bergström, L. M.; Pedersen, J. N.; Pedersen, J. S.; Hansson, P., Self-assembling properties of ionisable amphiphilic drugs in aqueous solution. *Journal of Colloid and Interface Science* **2021,** *600*, 701-710.
47. Attwood, D.; Agarwal, S. P.; Waigh, R. D., Effect of the nature of the hydrophobic group on the mode of association of amphiphilic molecules in aqueous solution. *Journal of the Chemical Society, Faraday Transactions 1: Physical Chemistry in Condensed Phases* **1980,** *76* (0), 2187-2193.
48. Attwood, D.; Udeala, O. K., Aggregation of antihistamines in aqueous solution: micellar properties of some diphenylmethane derivatives. *Journal of Pharmacy and Pharmacology* **1974,** *26* (11), 854-860.

49. GREEN, A. L., Ionization constants and water solubilities of some aminoalkylphenothiazine tranquillizers and related compounds. *Journal of Pharmacy and Pharmacology* **2011,** *19* (1), 10-16.
50. Embil, K.; Torosian, G., Solubility and ionization characteristics of doxepin and desmethyldoxepin. *J Pharm Sci* **1982,** *71* (2), 191-3.
51. AP, I. J., Limiting solubilities and ionization constants of sparingly soluble compounds: determination from aqueous potentiometric titration data only. *Pharm Res* **1988,** *5* (12), 772-5.
52. Dalmark, M.; Storm, H. H., A Fickian diffusion transport process with features of transport catalysis. Doxorubicin transport in human red blood cells. *J Gen Physiol* **1981,** *78* (4), 349-64.
53. Konop, A. J.; Colby, R. H., Role of condensed counterions in the thermodynamics of surfactant micelle formation with and without oppositely charged polyelectrolytes. *Langmuir* **1999,** *15*, 58-65.
54. Lindman, B.; Khan, A.; Marques, E.; Miguel, M.; Piculell, L.; Thalberg, K., Phase behavior of polymer-surfactant systems in relation to polymer-polymer and surfactant-surfactant mixtures. *Pure and Applied Chemistry.* **1993,** *65*, 953-958.
55. Goddard, E. D., Polymer-surfactant interaction. Part 2. Polymer and surfactant of opposite charge. *Colloids Surf.* **1986,** *19*, 301-29.
56. Chu, D.; Thomas, J. K., Effect of Cationic Surfactants on the Conformational Transition of Poly(methacrylic acid). *J. Am. Chem. Soc.* **1986,** *108*, 6270-76.
57. Hansson, P., Self-assembly of ionic surfactants in polyelectrolyte solutions: A model for mixtures of opposite charge. *Langmuir* **2001,** *17*, 4167-4180.
58. Khokhlov, A. R.; Kramarenko, E. Y.; Makhaeva, E. E.; Starodubtzev, S. G., Collapse of polyelectrolyte networks induced by their interaction with oppositely charged surfactants. *Macromolecules* **1992,** *25*, 4779-83.
59. Hansson, P.; Schneider, S.; Lindman, B., Phase separation in polyelectrolyte gels interacting with surfactants of opposite charge. *J. Phys. Chem. B* **2002,** *106*, 9777-9793.
60. Zaroslov, Y. D.; Philippova, O. E.; Khokhlov, A. R., Change of elastic modulus of strongly charged hydrogels at the collapse transition. *Macromolecules* **1999,** *32*, 1508-1513.
61. Dembo, A. T.; Yakunin, A. N.; Zaitsev, V. S.; Mironov, A. V.; Starodubtsev, S. G.; Khokhlov, A. R.; Chu, B., Regular microstructures in gel-surfactant complexes: Influence of water content and comparison with the surfactant structure in water. *J. Polym. Sci.: Part B: Polymer Physics* **1996,** *34*, 2893-2898.
62. Khokhlov, A.; Makhaeva, E. E.; Philippova, O. E.; Starodubtzev, S. G., Supramolecular structures and conformational transitions in polyelectrolyte gels. *Macromol. Symp.* **1994,** *87*, 69-91.
63. Khokhlov, A. R.; Starodubtzev, S. G.; Vasilevskaya, V. V., Conformational transitions in polymer gels: Theory and experiment. *Adv. Polym. Sci.* **1993,** *109*, 123-171.
64. Mironov, A. V.; Starodubtsev, S. G.; Khokhlov, A. R.; Dembo, A. T.; Dembo, K. A., Effect of chemical nature of 1,1-salt on structure of polyelectrolyte gel-surfactant complexes. *J. Phys. Chem. B* **2001,** *105*, 5612-5617.
65. Chen, Y. M.; Katsuyama, Y.; Gong, J. P.; Osada, Y., Influence of shear stress on cationic surfactant uptake by anionic gels. *J. Phys. Chem. B* **2003,** *107*, 13601-13607.
66. Gong, J. P.; Osada, Y., Theoretical analysis of the cross-linking effect on the polyelectrolyte-surfactant interaction. *J. Phys. Chem.* **1995,** *99*, 10971-5.

67. Narita, T.; Gong, J. P.; Osada, Y., Kinetic study of surfactant binding into polymer gel - Experimental and theoretical analyses. *J. Phys. Chem. B* **1998,** *102*, 4566-4572.
68. Narita, T.; Hirota, N.; Gong, J. P.; Osada, Y., Effects of counterions and co-ions on the surfactant binding process in the charged polymer network. *J. Phys. Chem. B* **1999,** *103*, 6262-6266.
69. Okuzaki, H.; Osada, Y., Role and effect of cross-linkage on the polyelectrolyte-surfactant interaction. *Macromolecules* **1995,** *28*, 4554-7.
70. Sasaki, S.; Koga, S., Order-disorder phase transition of polyelectrolyte gel-surfactant complexes. *Macromolecules* **2004,** *37*, 3809-3814.
71. Sasaki, S.; Koga, S.; Imabayashi, R.; Maeda, H., Salt effects on the volume transition of ionic gel induced by the hydrophobic counterion binding. *J. Phys. Chem. B* **2001,** *105*, 5852-5855.
72. Lynch, I.; Sjöström, J.; Piculell, L., Reswelling of polyelectrolyte hydrogels by oppositely charged surfactants. *J. Phys. Chem. B* **2005,** *109*, 4258-4262.
73. Karabanova, V. B.; Rogacheva, V. B.; Zezin, A. B.; Kabanov, V. A., Interaction of cross-linked sodium polyacrylate with proteins. *Polymer Science* **1995,** *37*, 1138-1143.
74. Khandurina, Y. V.; Rogacheva, V. B.; Zezin, A. B.; Kabanov, V. A., Interaction of cross-linked polyelectrolytes with oppositely charged surfactants. *Polym. Sci.* **1994,** *36*, 184-188.
75. Zezin, A. B.; Rogacheva, V.; Skobeleva, V.; Kabanov, V., Controlled uptake and release of proteins by polyelectrolyte gels. *Polym. Adv. Technol.* **2002,** *13*, 919-925.
76. Andersson, M.; Hansson, P., Phase Behavior of Salt-Free Polyelectrolyte Gel–Surfactant Systems. *J. Phys. Chem. B* **2017,** *121* (24), 6064-6080.
77. Hansson, P., Interaction between polyelectrolyte gels and surfactants of opposite charge. *Curr. Opin. Colloid Interface Sci.* **2006,** *11*, 351-362.
78. Hansson, P., Surfactant self-assembly in oppositely charged polymer networks. Theory. *J. Phys. Chem. B* **2009,** *113*, 12903-12915.
79. Hansson, P.; Schneider, S.; Lindman, B., Macroscopic phase separation in a polyelectrolyte gel interacting with oppositely charged surfactant: correlation between anomalous deswelling and microstructure. *Prog. Colloid Polym. Sci.* **2000,** *115*, 342-346.
80. Johansson, C.; Hansson, P., Distribution of cytochrome c in polyacrylate microgels. *Soft Matter* **2010,** *6*, 3970-3978.
81. Nilsson, P.; Hansson, P., Regular and Irregular deswelling of polyacrylate and hyaluronate gels induced by oppositely charged surfactants. *J. Colloid Int. Sci.* **2008,** *325*, 316-323.
82. Nilsson, P.; Hansson, P., Deswelling kinetics of polyacrylate gels in solutions of cetyltrimethylammunium bromide. *J. Phys. Chem. B* **2007,** *111*, 9770-9778.
83. Nilsson, P.; Unga, J.; Hansson, P., Effect of salt and surfactant concentration on the structure of polyacrylate gel/surfactant complexes. *J. Phys. Chem. B* **2007,** *111*, 10959-10964.
84. Gernandt, J.; Frenning, G.; Richtering, W.; Hansson, P., A model describing the internal structure of core/shell hydrogels. *Soft Matter* **2011,** *7*, 10327.
85. Gernandt, J.; Hansson, P., Surfactant-induced core/shell phase equilibrium in hydrogels. *J. Chem. Phys.* **2016,** *144*, 064902.
86. Nilsson, P.; Hansson, P., Ion-exchange controls the kinetics of deswelling of polyelectrolyte microgels in solutions of oppositely charged surfactant. *J. Phys. Chem. B* **2005,** *109*, 23843-23856.

87. Jidheden, C.; Hansson, P., Single microgels in core-shell equilibrium: A novel method for limited volume studies. *J. Phys. Chem. B* **2016,** *120*, 10030-10042.
88. Gernandt, J.; Hansson, P., Core-shell separation of a hydrogel in a large solution of proteins. *Soft Matter* **2012,** *8*, 10905-10913.
89. Khokhlov, A. R.; Kramarenko, E. Y.; Makhaeva, E. E.; Starodoubtzev, S. G., Collapse of polyelectrolyte networks induced by their interaction with an oppositely charged surfactant. Theory. *Makromol. Chem. Theory Simul.* **1992,** *1*, 105-18.
90. Xiao, X.; Ji, J.; Zhao, W.; Nangia, S.; Libera, M., Salt Destabilization of Cationic Colistin Complexation within Polyanionic Microgels. *Macromolecules* **2022,** *55* (5), 1736-1746.
91. Hansson, P., Volume transition and phase coexistence in polyelectrolyte gels interacting with amphiphiles and proteins. *Gels* **2020,** *6*, 24.
92. Kabanov, V. A.; Zezin, A. B.; Rogacheva, V. B.; Khandurina, Y. V., Absorption of ionic amphiphils by oppositely charged polyelectrolytes. *Macromol. Symp.* **1997,** *126*, 79-94.
93. Gernandt, J.; Hansson, P., Hysteresis in the surfactant-induced volume transition of hydrogels. *J. Phys. Chem. B* **2015,** *119*, 1717-1725.
94. Granfeldt, M. K.; Jönsson, B.; Woodward, C. E., A Monte Carlo study of the interaction between charged colloids carrying adsorbed polyelectrolytes. *J. Phys. Chem.* **1991,** *95*, 4819-4826.
95. Svensson, A.; Piculell, L.; Karlsson, L.; Cabane, B.; Jönsson, B., Phase behavior of an ionic surfactant with mixed monovalent/polymeric counterions. *J. Phys. Chem. B* **2003,** *107*, 8119-8130.
96. Onuki, A., Paradox in phase transitions with volume change. *Phys. Rev. A* **1988,** *38*, 2192-2195.
97. Wang, G.; Li, M.; Chen, X., Inverse suspension polymerization of sodium acrylate. *Journal of Applied Polymer Science* **1997,** *65* (4), 789-794.
98. Svergun, D. I.; Koch, M. H. J.; Timmins, P. A.; May, R. P., *Small Angle X-Ray and Neutron Scattering from Solutions of Biological Macromolecules: Small Angle X-Ray and Neutron Scattering from Biomacromolecular Solutions*. Oxford University Press, Incorporated: Oxford, 2013.
99. Kotlarchyk, M.; Chen, S. H., Analysis of small angle neutron scattering spectra from polydisperse interacting colloids. *The Journal of Chemical Physics* **1983,** *79* (5), 2461-2469.
100. Berr, S. S., Solvent isotope effects on alkytrimethylammonium bromide micelles as a function of alkyl chain length. *The Journal of Physical Chemistry* **1987,** *91* (18), 4760-4765.
101. Hayter, J. B.; Penfold, J., An analytic structure factor for macroion solutions. *Molecular Physics* **1981,** *42* (1), 109-118.
102. Hansen, J.-P.; Hayter, J. B., A rescaled MSA structure factor for dilute charged colloidal dispersions. *Molecular Physics* **1982,** *46* (3), 651-656.
103. Hollricher, O., Raman Instrumentation for Confocal Raman Microscopy. In *Confocal Raman Microscopy*, Toporski, J.; Dieing, T.; Hollricher, O., Eds. Springer International Publishing: Cham, 2018; pp 69-87.
104. Hansson, P., Self-assembly of ionic surfactant in cross-linked polyelectrolyte gel of opposite charge. A physical model for highly charged systems. *Langmuir* **1998,** *14*, 2269-2277.
105. Israelachvili, J. N., *Intermolecular and Surface Forces*. 2nd ed.; Academic Press Limited: London, 1992.

106. Biondi, M.; Fusco, S.; Lewis, A. L.; Netti, P. A., New insights into the mechanisms of the interactions between doxorubicin and the ion-exchange hydrogel DC Bead™ for use in transarterial chemoembolization (TACE). *J Biomater Sci Polym Ed* **2012,** *23* (1-4), 333-54.
107. Biondi, M.; Fusco, S.; Lewis, A. L.; Netti, P. A., Investigation of the mechanisms governing doxorubicin and irinotecan release from drug-eluting beads: mathematical modeling and experimental verification. *J Mater Sci Mater Med* **2013,** *24* (10), 2359-70.
108. Gonzalez, M. V.; Tang, Y.; Phillips, G. J.; Lloyd, A. W.; Hall, B.; Stratford, P. W.; Lewis, A. L., Doxorubicin eluting beads-2: methods for evaluating drug elution and in-vitro:in-vivo correlation. *J Mater Sci Mater Med* **2008,** *19* (2), 767-75.
109. Fülöp, Z.; Gref, R.; Loftsson, T., A permeation method for detection of self-aggregation of doxorubicin in aqueous environment. *Int J Pharm* **2013,** *454* (1), 559-61.
110. Ashbaugh, H. S.; Lindman, B., Swelling and structural changes of oppositely charged polyelectrolyte gel-mixed surfactant complexes. *Macromolecules* **2001,** *34*, 1522-1525.

Acta Universitatis Upsaliensis

Digital Comprehensive Summaries of Uppsala Dissertations from the Faculty of Pharmacy 312

Editor: The Dean of the Faculty of Pharmacy

A doctoral dissertation from the Faculty of Pharmacy, Uppsala University, is usually a summary of a number of papers. A few copies of the complete dissertation are kept at major Swedish research libraries, while the summary alone is distributed internationally through the series Digital Comprehensive Summaries of Uppsala Dissertations from the Faculty of Pharmacy. (Prior to January, 2005, the series was published under the title "Comprehensive Summaries of Uppsala Dissertations from the Faculty of Pharmacy".)

Distribution: publications.uu.se
urn:nbn:se:uu:diva-472818

ACTA
UNIVERSITATIS
UPSALIENSIS
UPPSALA
2022